Internal waves in the atmosphere and ocean

Oliver Bühler
Alexander Hasha
Caroline Muller
Miranda Holmes-Cerfon
Marija Vucelja

Courant Institute of Mathematical Sciences
Department of Mathematics
Center for Atmosphere Ocean Science

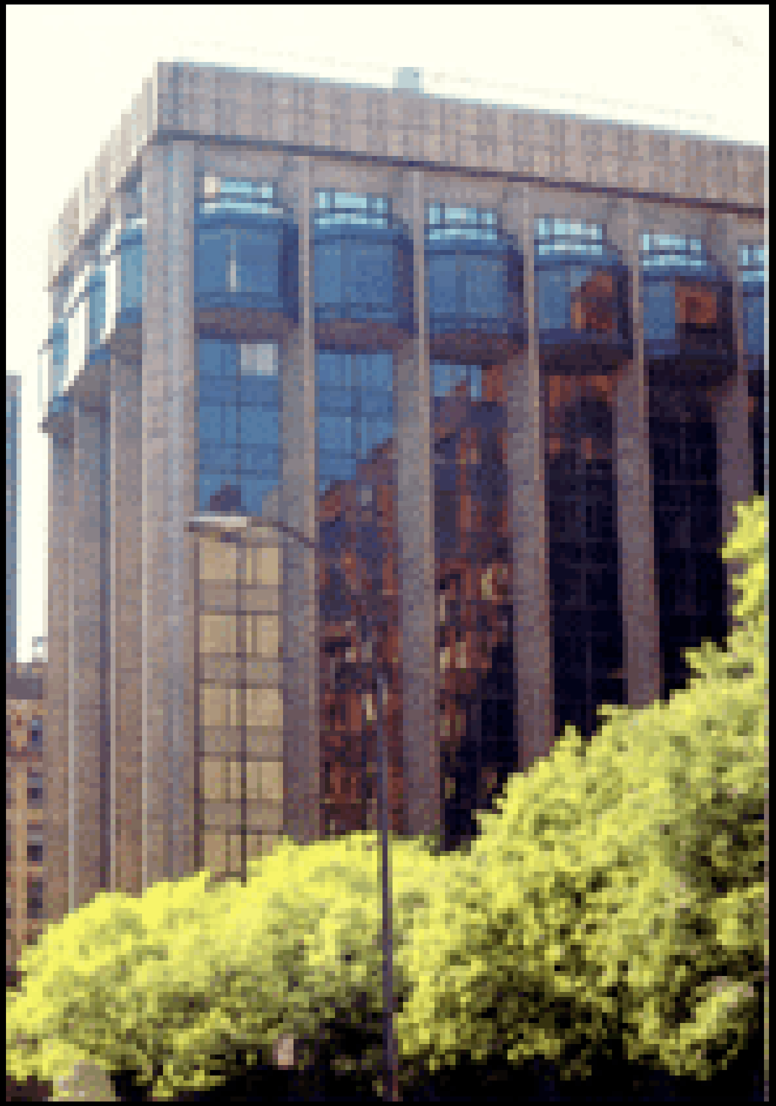

Interdisciplinary PhD program in
Atmosphere Ocean Science and Mathematics

New York University

Atmosphere and ocean conditions

Atmosphere:

Waves are mostly generated near ground with large range of scales (eg horizontal wavelengths from very small to over 1000km).
Propagation upwards, strong mean flow refraction (10 m/s) and density decay effects. Inevitable wave breaking.
Life cycle is nasty, brutish, and short.
Importance mostly due to wave-induced vertical transport of angular momentum.

Ocean:

Wave generation at top and bottom, horizontal scale limited to about 150km (ie mode 1).
Propagation upwards and downwards, weaker mean flow refraction (10cm/s), no density decay effects. Eventually intermittent wave breaking.
Life cycle is much longer and interaction effects can add up. Importance mostly due to wave-induced vertical mixing by 3d turbulence during breaking.

Simulation in GCMs:

Balanced vortical flow in atmosphere mostly at resolvable synoptic scale (1000km), in ocean the same scale (“mesoscale”) is at unresolvable 50km. Ray tracing works poorly in ocean models. Gravity-wave-permitting vs. eddy-permitting.

Need to parametrize wave effects is acute in both systems, but
there are no gw parametrizations in current ocean gcms
(vertical mixing included by fixed global diffusivity parameter)

There is scope for improvement by comparing experiences in both fields

Rocking like Chapman 2004

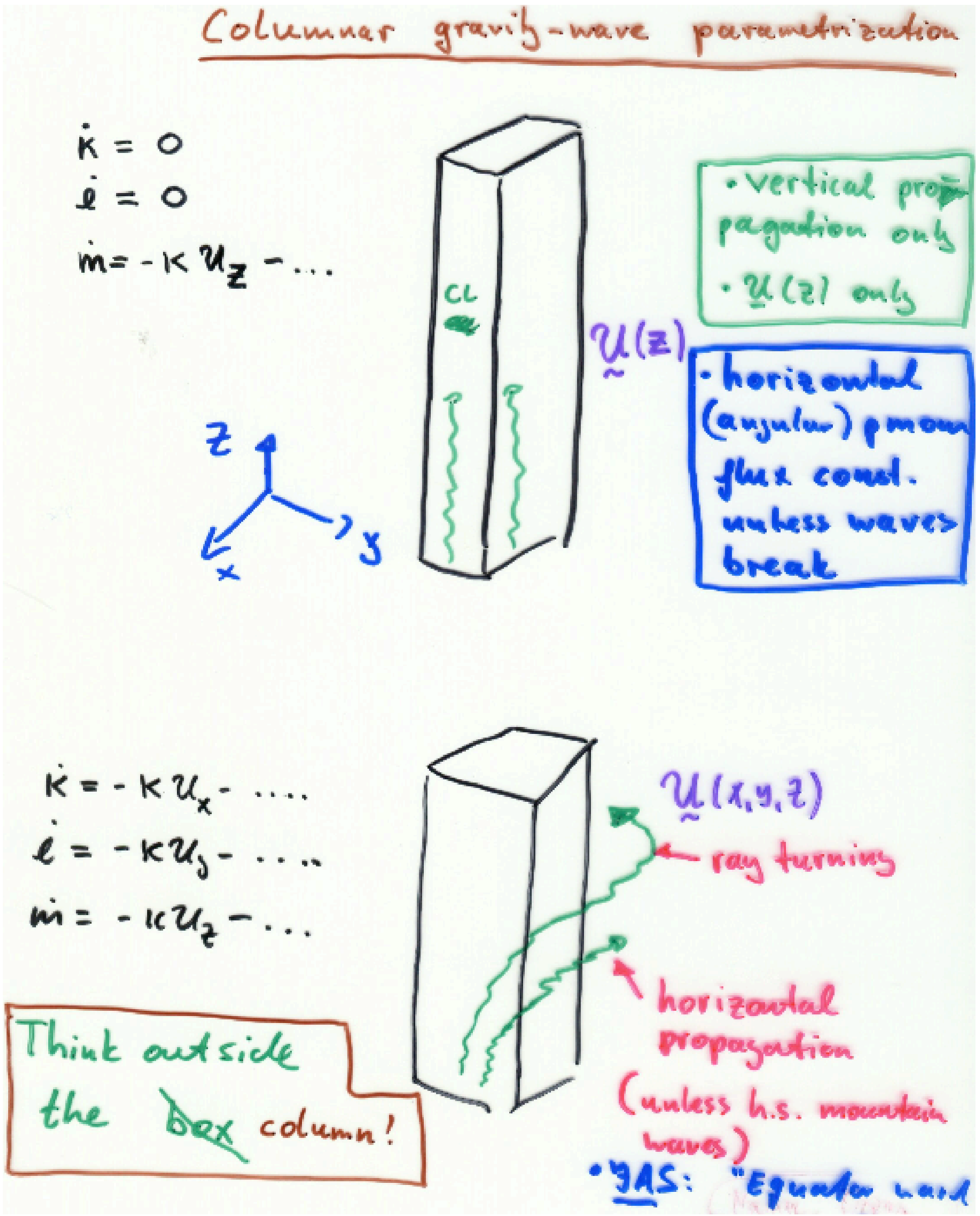

Columnar gravity-wave parametrizations common in all atmospheric GCMs.

No GW parametrizations at all in ocean models, just a numerical value for a wave-induced vertical diffusivity.

Columnar parametrization: Parametrization is applied independently in each vertical model column. Track pseudomomentum flux.

Bühler, JAS 2003
Meridional propagation of GWs, signature in kinetic and potential energy

Bühler & McIntyre, JFM, 2003 + 2005
“Remote recoil” and “wave capture”

3d ray tracing and wave-mean interaction

Wavepackets along group-velocity ray

Wavepackets are the fundamental solutions of ray tracing

Wavetrains can be built from wavepackets

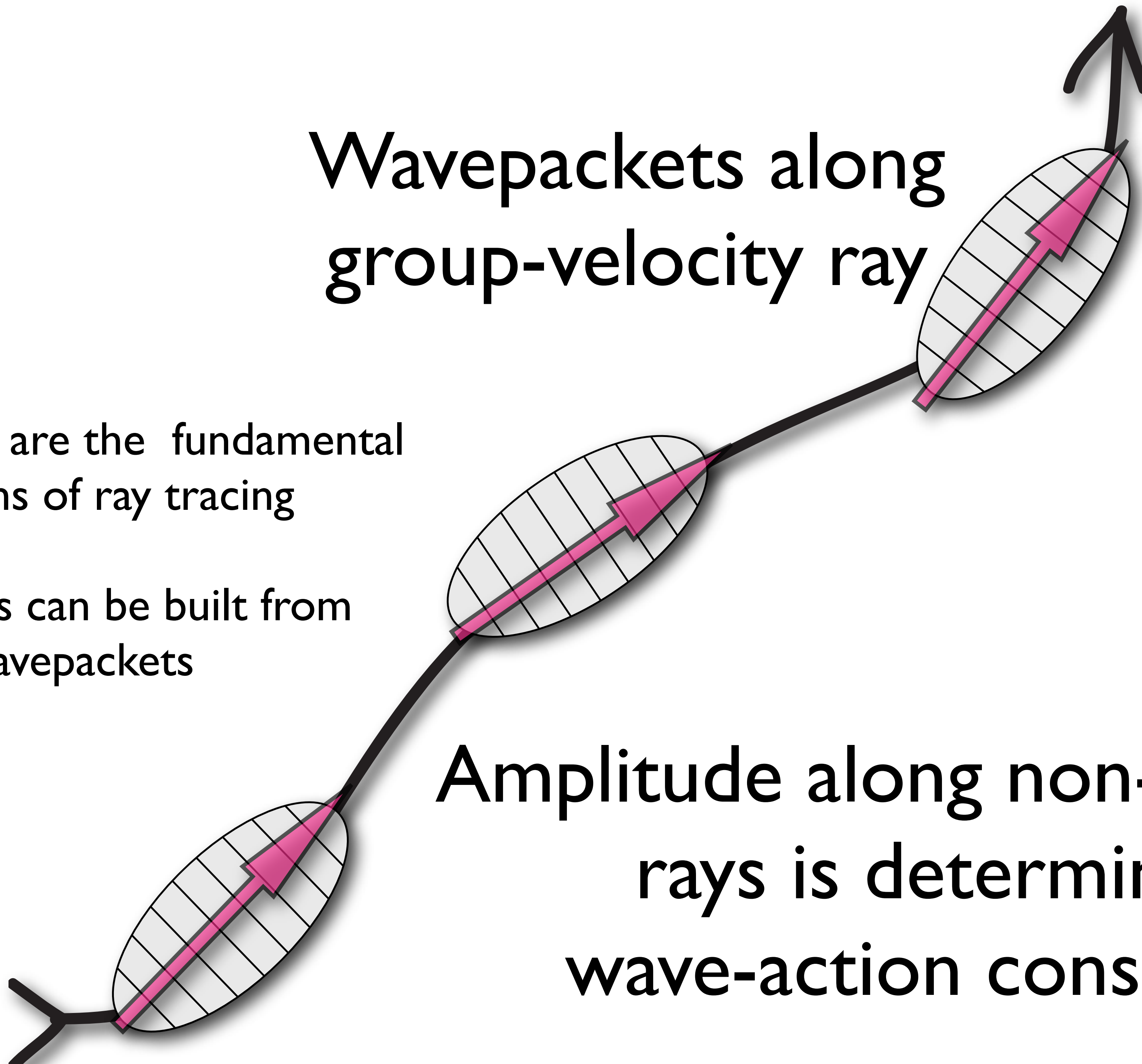

Amplitude along non-intersecting rays is determined by wave-action conservation

3d ray tracing for position and wavenumber

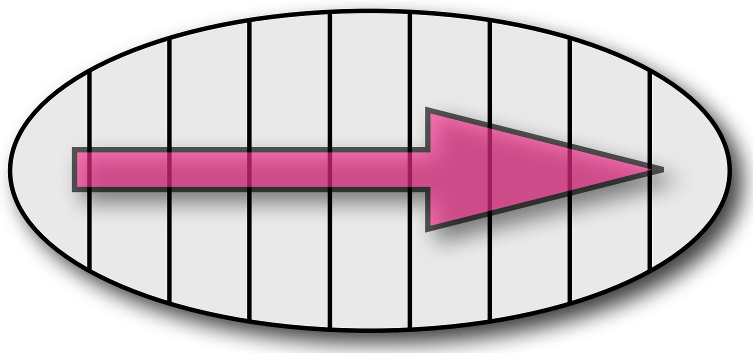

phase lines
of a wavepacket

$$\Omega(\boldsymbol{k}, \boldsymbol{x}, t) = \boldsymbol{U} \cdot \boldsymbol{k} + \hat{\omega}$$

$$\boxed{\frac{\mathrm{d}\boldsymbol{x}}{\mathrm{d}t} = +\frac{\partial \Omega}{\partial \boldsymbol{k}} \quad \text{and} \quad \frac{\mathrm{d}\boldsymbol{k}}{\mathrm{d}t} = -\frac{\partial \Omega}{\partial \boldsymbol{x}}}$$

Group velocity

$$\boldsymbol{u}_g = \frac{\mathrm{d}\boldsymbol{x}}{\mathrm{d}t} = \boldsymbol{U} + \hat{\boldsymbol{u}}_g$$

Ray time derivative

$$\frac{\mathrm{d}}{\mathrm{d}t} = \frac{\partial}{\partial t} + (\boldsymbol{u}_g \cdot \boldsymbol{\nabla})$$

Simple case $\hat{\omega}(\boldsymbol{k})$:

$$\boxed{\frac{\mathrm{d}k_i}{\mathrm{d}t} = -\frac{\partial U_j}{\partial x_i} k_j}$$

Wavenumber changes
due to background
inhomogeneity
--> refraction

Wave action and pseudomomentum

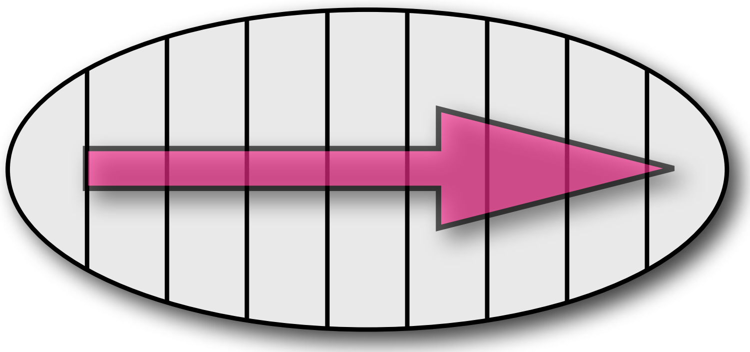

"Mean" is the average
over rapidly varying
wave phase

$$h = \overline{h} + h'$$
$$\overline{h'} = 0$$

Wave energy $$E = \frac{1}{2}\left(H\overline{|\boldsymbol{u}'|^2} + g\overline{h'^2}\right)$$ Example in shallow water

Wave action $$A = \frac{E}{\hat{\omega}}$$

Bretherton & Garrett 1968

$$\boxed{\frac{\partial A}{\partial t} + \boldsymbol{\nabla}\cdot(A\boldsymbol{u}_g) = 0}$$

Amplitude prediction from
scalar wave action <u>conservation</u>

Important
vector wave property:

$\boxed{\text{Pseudomomentum } \mathbf{p} = \boldsymbol{k}\, A}$ 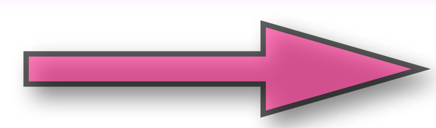

Pseudomomentum <u>changes</u> with wavenumber
due to refraction

Understanding wavenumber refraction

Wavenumber

$$\frac{\mathrm{d}k_{\underline{i}}}{\mathrm{d}t} = -\frac{\partial U_j}{\partial x_{\underline{i}}} k_j$$ is equivalent to $$\boxed{\frac{\mathrm{d}\boldsymbol{k}}{\mathrm{d}t} = -\boldsymbol{\nabla}\boldsymbol{U} \cdot \boldsymbol{k}}$$

Passive tracer

$\phi(\boldsymbol{x}, t)$ such that

$$\mathrm{D}_t\phi = 0$$

$$\boxed{\mathrm{D}_t\left(\boldsymbol{\nabla}\phi\right) = -\boldsymbol{\nabla}\boldsymbol{U} \cdot \left(\boldsymbol{\nabla}\phi\right)}$$

$\boldsymbol{k}$ and $\boldsymbol{\nabla}\phi$ evolve similarly

(i.e. wave phase and passive tracer evolve similarly)

Intrinsic difference

$$\boldsymbol{u}_g = \frac{\mathrm{d}\boldsymbol{x}}{\mathrm{d}t} = \boldsymbol{U} + \hat{\boldsymbol{u}}_g$$

$$\boxed{\frac{\mathrm{d}}{\mathrm{d}t} - \mathrm{D}_t = \left(\hat{\boldsymbol{u}}_g \cdot \boldsymbol{\nabla}\right)}$$

measures the misfit

Wavepacket exposed to pure strain in analogy with passive advection

$\mathbf{p} = \boldsymbol{k}\, A$

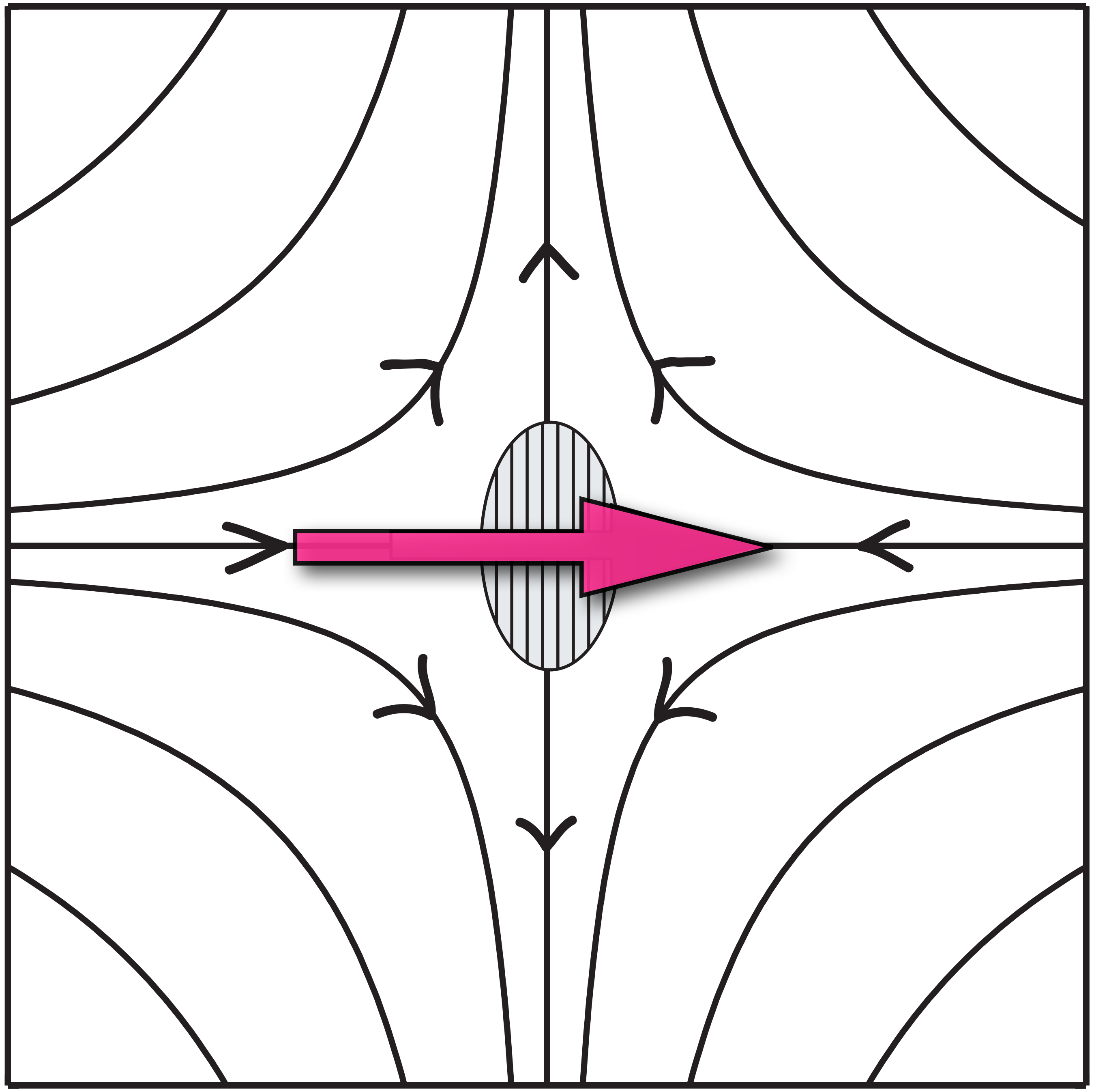

Wavepacket is squeezed in x and stretched in y. Action is constant

Wavenumber vector **k** is increases in size

Pseudomomentum **p** increases as well

Wave capture

Jones 1969, Badulin & Shira 1993, B&M 03,05

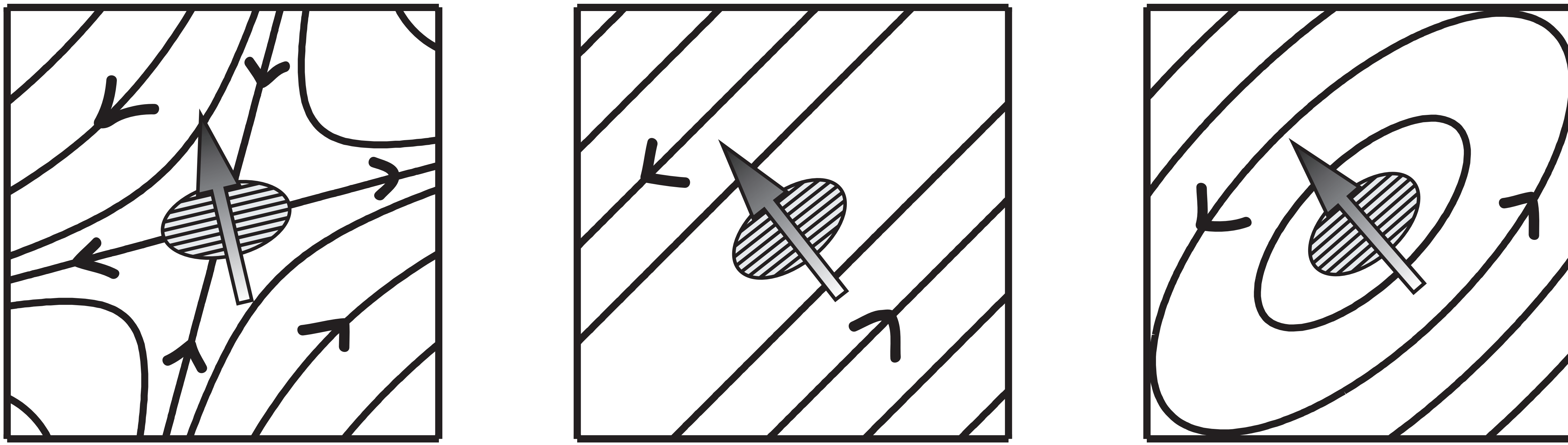

Hyperbolic D>0 | Parabolic D=0 | Elliptic D<0

The horizontal wavenumber vector aligns itself with the growing eigenvector, which is perpendicular to the extension axis

Pseudomomentum of the wavepacket changes
Grows exponentially in long run

Wave capture

Jones 1969, Badulin & Shira 1993, B&M 03,05

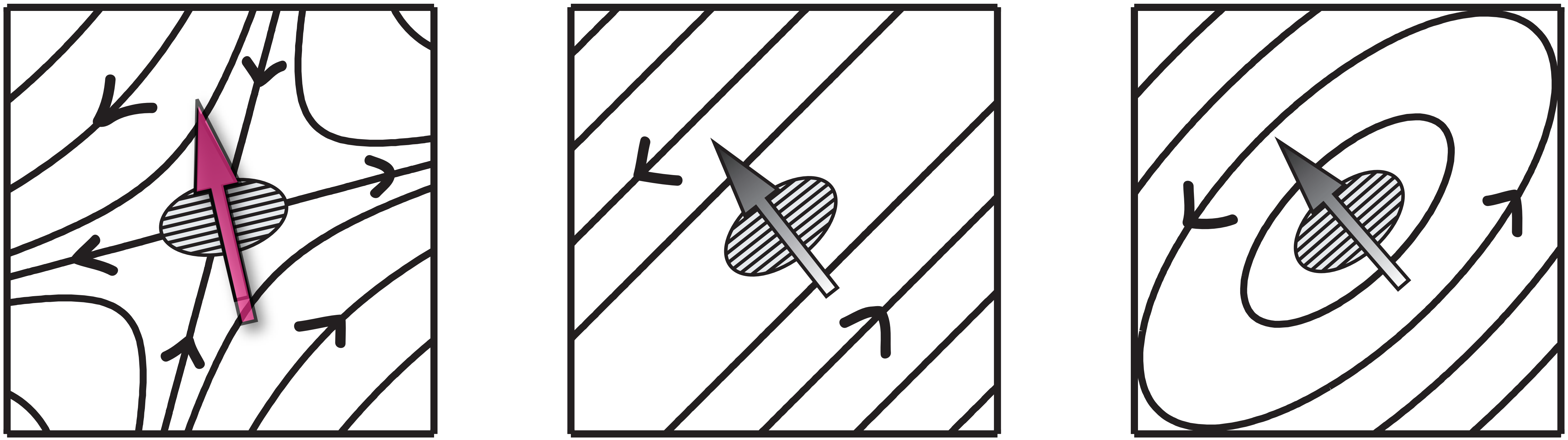

Hyperbolic D>0 Parabolic D=0 Elliptic D<0

The horizontal wavenumber vector aligns itself with the growing eigenvector, which is perpendicular to the extension axis

Pseudomomentum of the wavepacket changes
Grows exponentially in long run

Numerical example

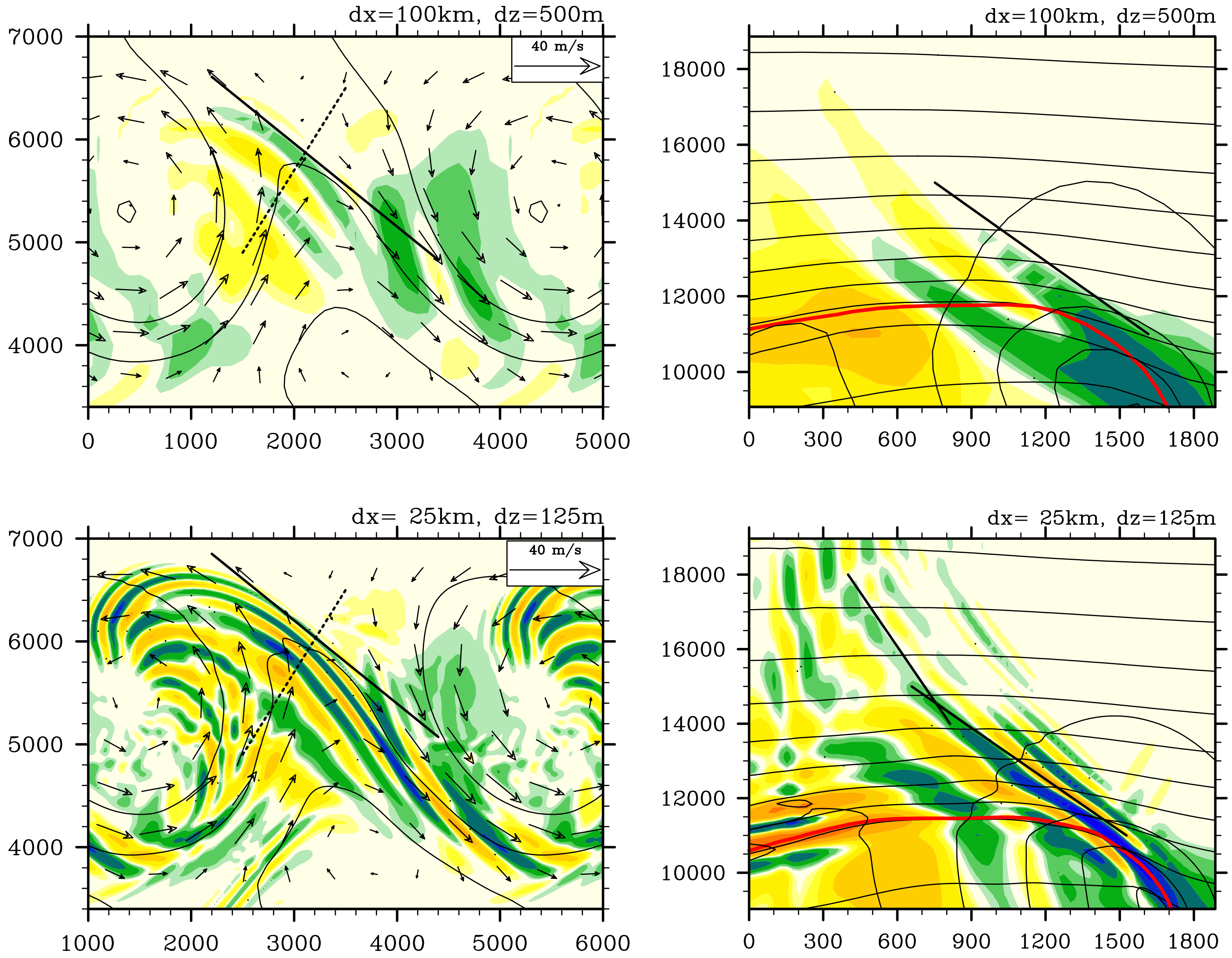

Plougonven & Snyder
GRL, 2005

Snapshots taken from numerical simulation of meandering jet stream

Interpreted based on wave straining

Back-reaction on the mean flow?

Remote recoil

Add a background vortex

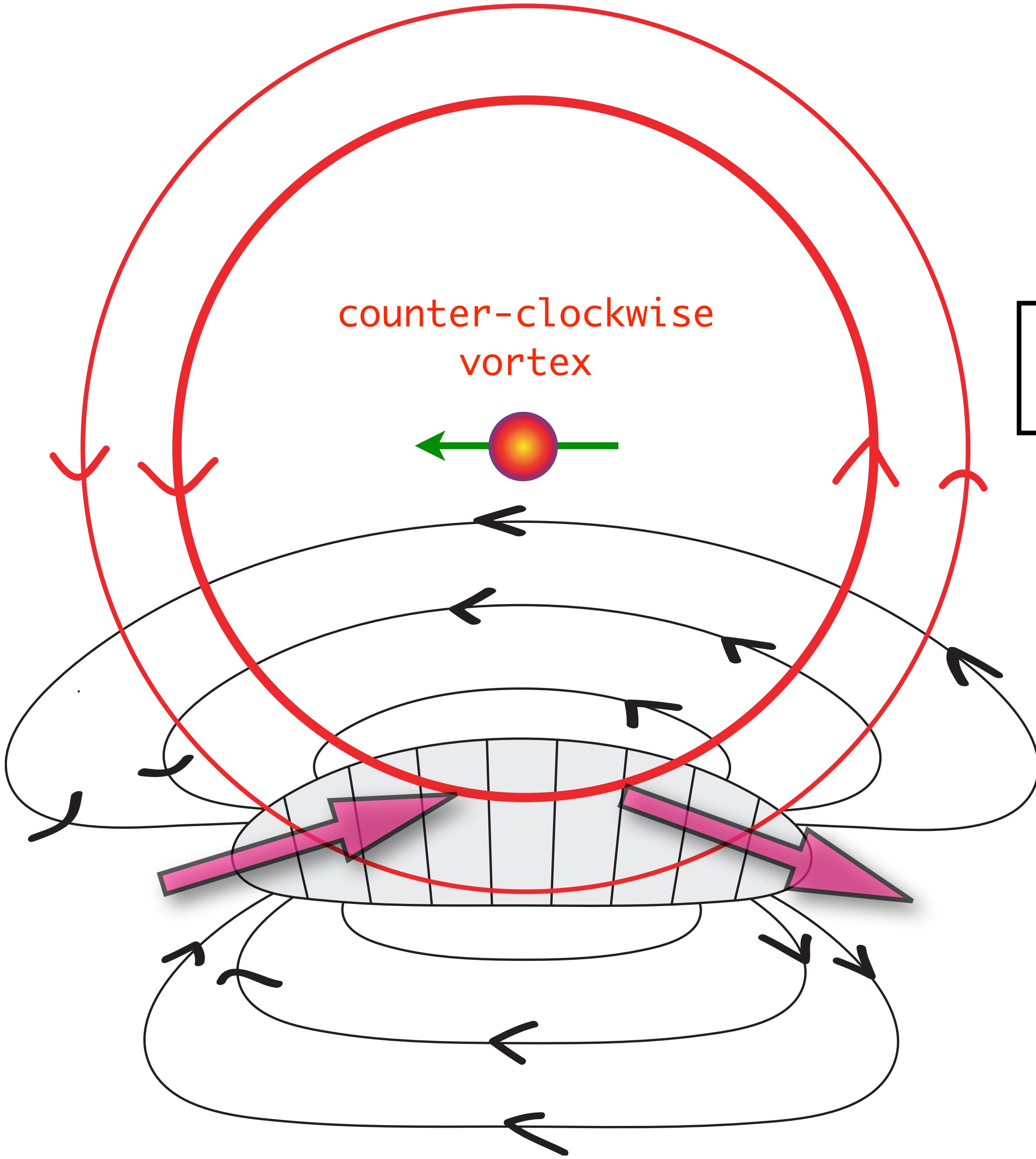

Bühler & McIntyre, JFM 03

A wavepacket can exchange momentum with a vortex without dissipating

Vortex-pair refraction

Pseudomomentum $\mathbf{p} = \boldsymbol{k}\, A$

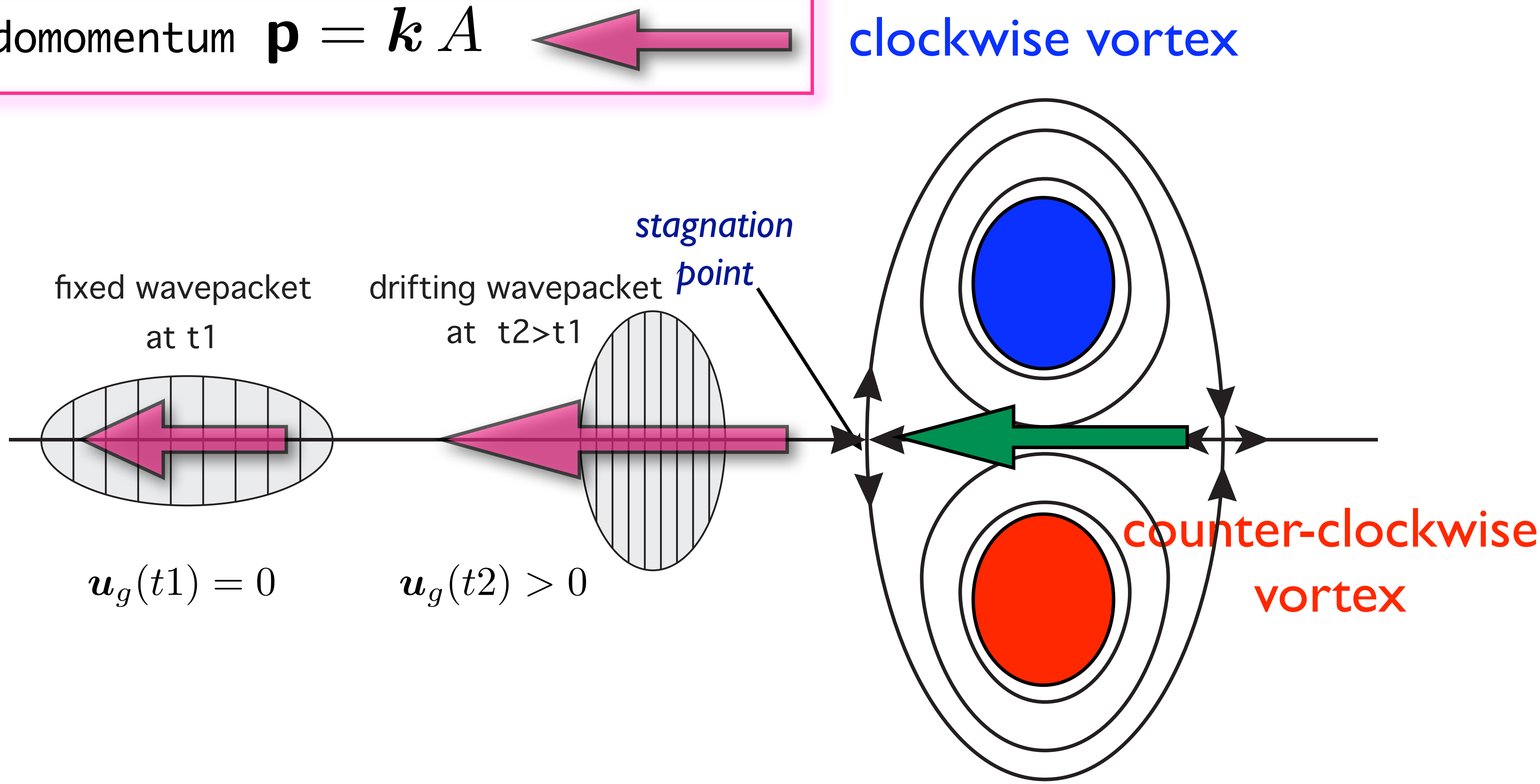

Vortex-pair refraction

Pseudomomentum $\mathbf{p} = \boldsymbol{k}\,A$

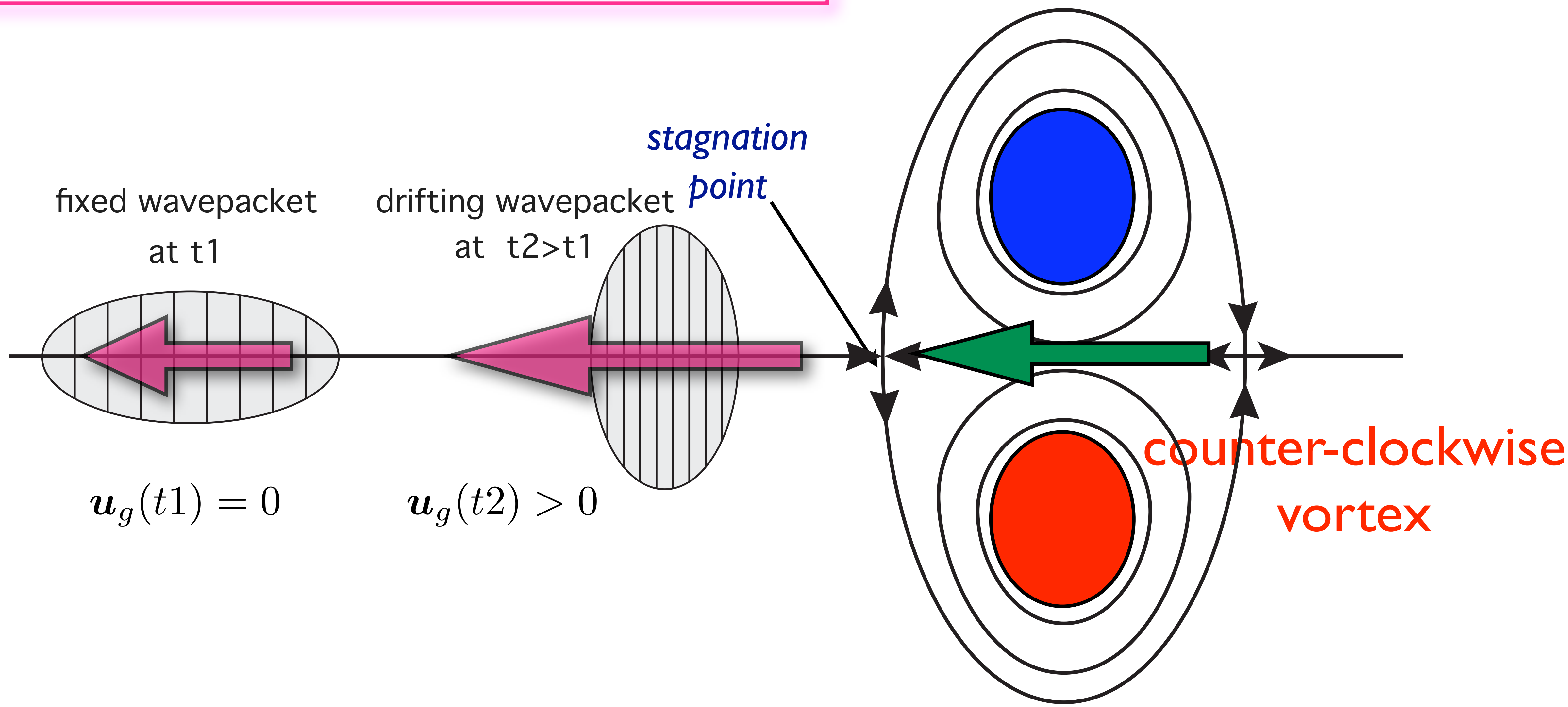

Pseudomomentum grows as wavepacket is compressed
Exchange of pmom and impulse, what about energy?

Energy transfer

Bühler & McIntyre, 2005

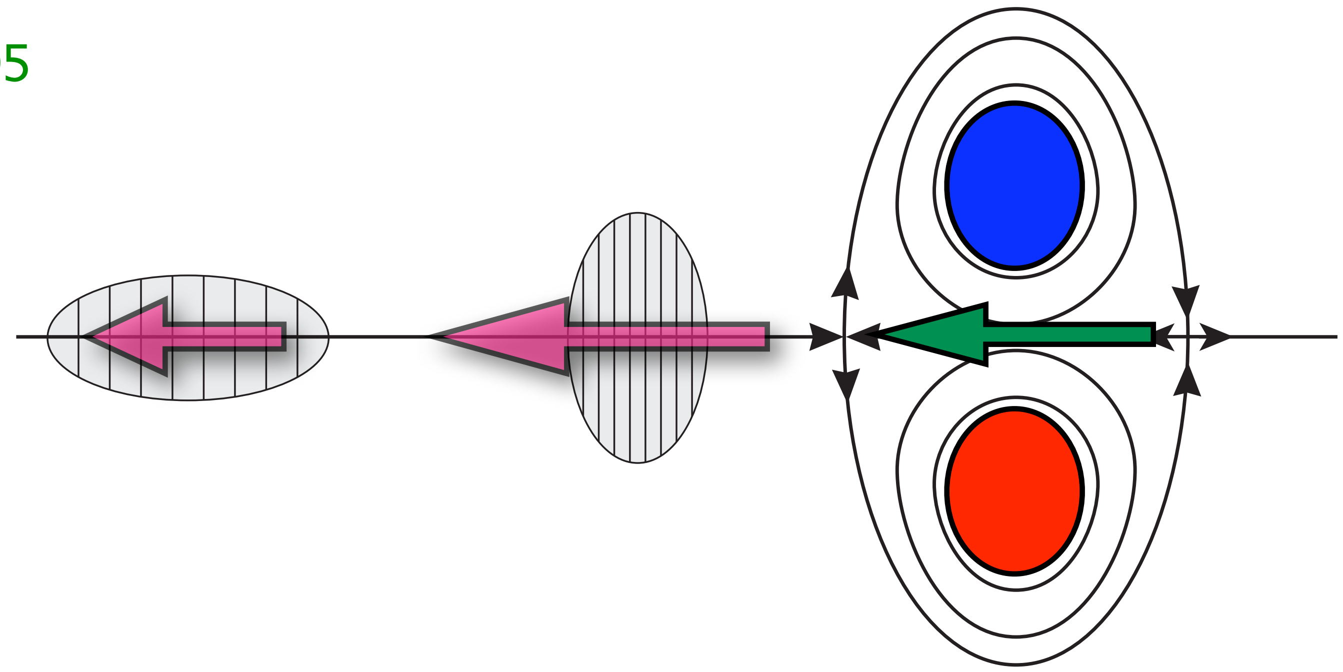

Action conservation

$$\frac{d}{dt}\int \frac{E}{\hat{\omega}}\, dxdy = 0$$

Refraction

$$\frac{d\hat{\omega}}{dt} = \sqrt{gH}\,\frac{d|\boldsymbol{k}|}{dt} > 0$$

Energy transfer:

$$\boxed{\frac{d}{dt}\int E\, dxdy > 0}$$

Wave-vortex energy transfer

Also wave-wave transfer as scale changes

Energy transfer

Bühler & McIntyre, 2005

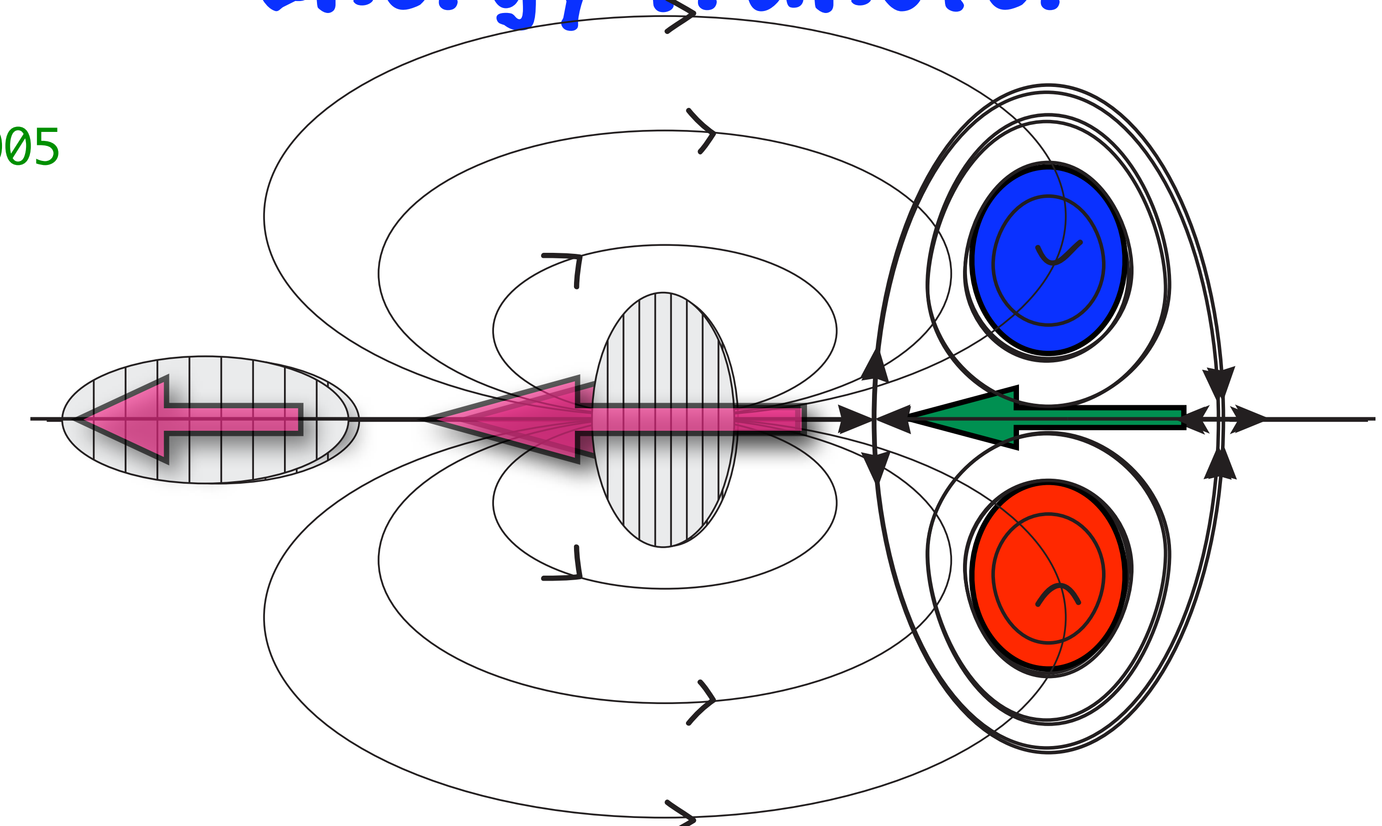

Action conservation

$$\frac{d}{dt}\int \frac{E}{\hat{\omega}}\,dxdy = 0$$

Refraction

$$\frac{d\hat{\omega}}{dt} = \sqrt{gH}\,\frac{d|\boldsymbol{k}|}{dt} > 0$$

Energy transfer:

$$\boxed{\frac{d}{dt}\int E\,dxdy > 0}$$

Wave-vortex energy transfer

Also wave-wave transfer as scale changes

Meanwhile in the ocean

NOVEMBER 2008 POLZIN

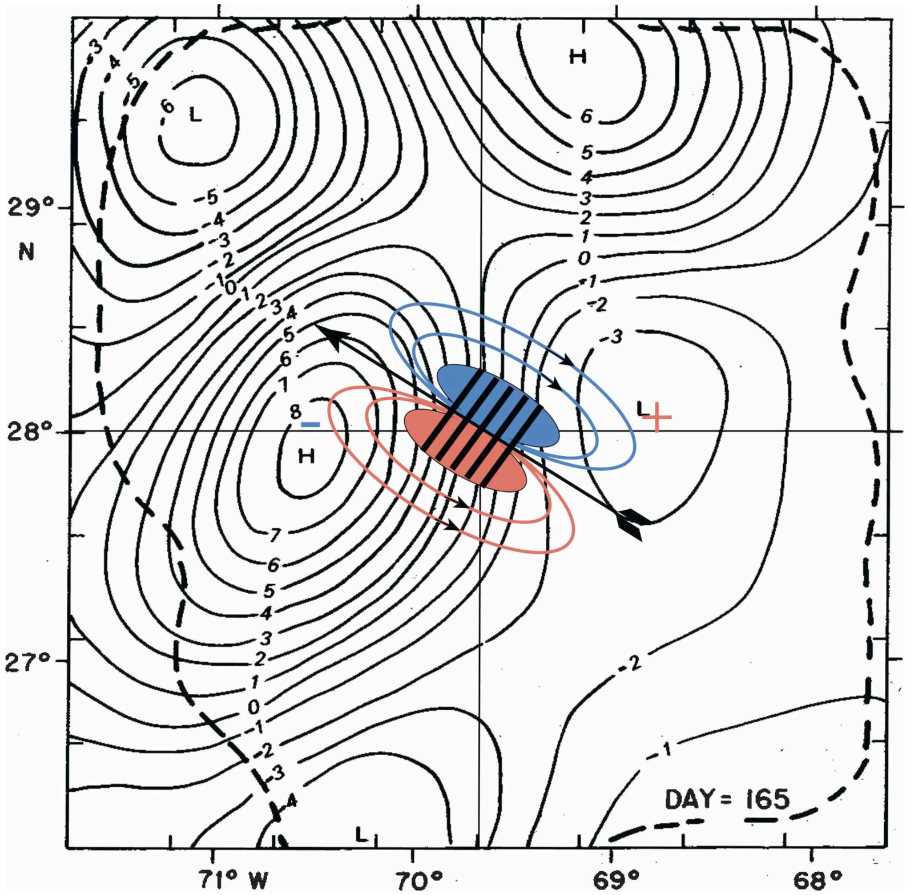

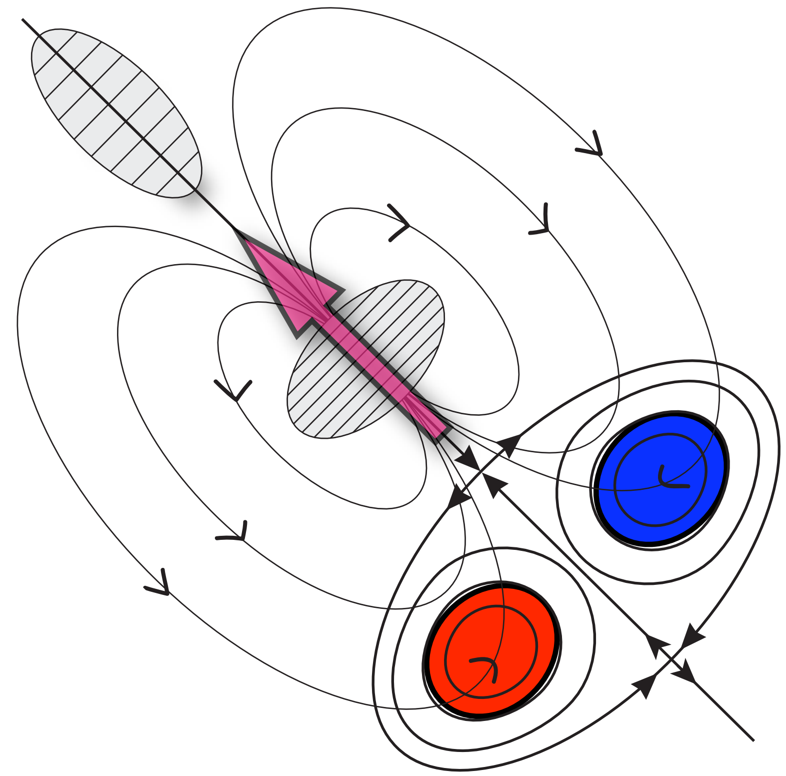

Polzin JPO 2008 data re-analysis of the Mid-Ocean Dynamics Experiment looks at fits with wave capture caused by mesoscale vortices

Could provides an energy sink mechanism for the mesoscale vortical flow but there really is no spatial scale separation for these flows.

Ray tracing is not enough.

3d refraction in the atmosphere

Gravity Wave Refraction by Three-Dimensionally Varying Winds and the Global Transport of Angular Momentum

ALEXANDER HASHA AND OLIVER BÜHLER

Courant Institute of Mathematical Sciences, New York, New York

JOHN SCINOCCA

Canadian Centre for Climate Modelling and Analysis, University of Victoria, Victoria, British Columbia, Canada

(Manuscript received 11 July 2007, in final form 8 January 2008)

ABSTRACT

Operational gravity wave parameterization schemes in GCMs are columnar; that is, they are based on a ray-tracing model for gravity wave propagation that neglects horizontal propagation as well as refraction by horizontally inhomogeneous basic flows. Despite the enormous conceptual and numerical simplifications that these approximations provide, it has never been clearly established whether horizontal propagation and refraction are indeed negligible for atmospheric climate dynamics. In this study, a three-dimensional ray-tracing scheme for internal gravity waves that allows wave refraction and horizontal propagation in spherical geometry is formulated. Various issues to do with three-dimensional wave dynamics and wave–mean interactions are discussed, and then the scheme is applied to offline computations using GCM data and launch spectra provided by an operational columnar gravity wave parameterization scheme for topographic waves. This allows for side-by-side testing and evaluation of momentum fluxes in the new scheme against those of the parameterization scheme. In particular, the wave-induced vertical flux of angular momentum is computed and compared with the predictions of the columnar parameterization scheme. Consistent with a scaling argument, significant changes in the angular momentum flux due to three-dimensional refraction and horizontal propagation are confined to waves near the inertial frequency.

Direct ray tracing tests

Part of PhD project Alex Hasha

As part of Alex's thesis we sought to adapt an existing ray-tracing scheme (GROGRAT) for atmospheric internal waves to test the impact of 3d refraction on the net wave-induced transport of angular momentum into the middle atmosphere

This turned out to be harder than we thought....

Ray tracing on a sphere is hard...

For instance, in a still, non-rotating atmosphere

waves should travel on great circles

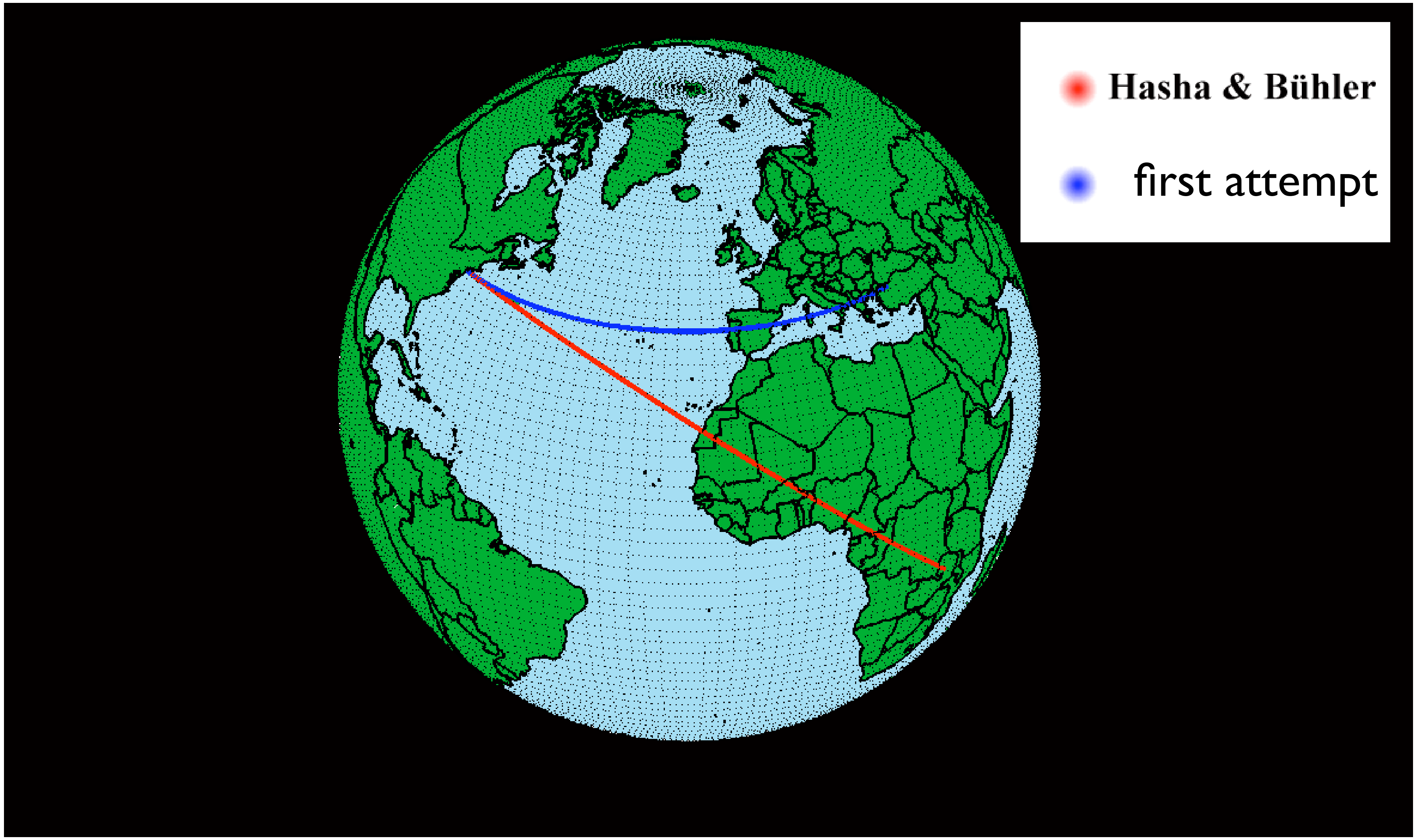

Low-frequency wave: strong effect

omega = 2f

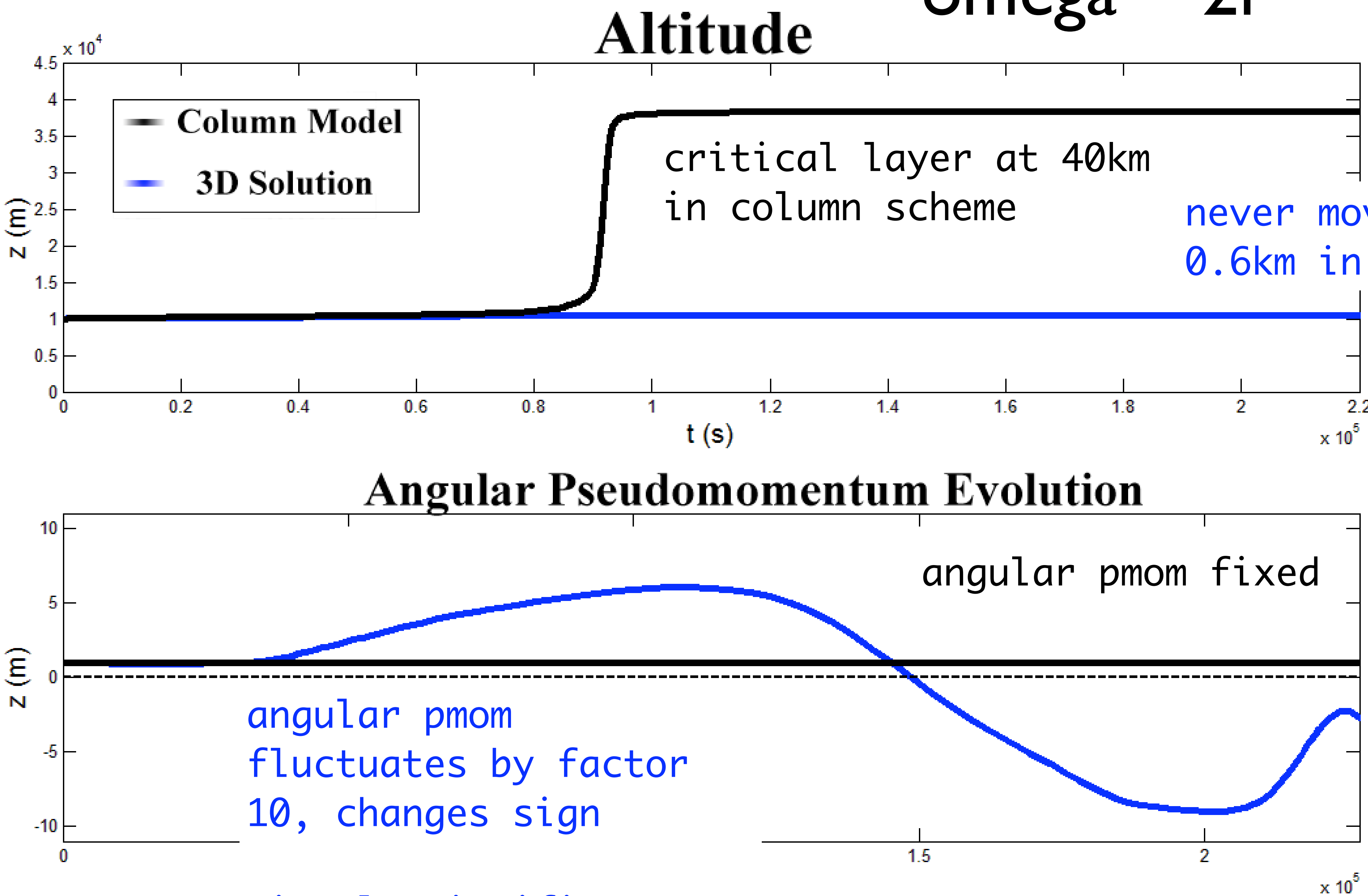

critical layer at 40km
in column scheme

never moves more than
0.6km in the vertical

angular pmom fixed

angular pmom
fluctuates by factor
10, changes sign

signals significant
interaction with mean
flow

High-frequency wave: weak effect

Eastward track launched at z=20km over NYC in winter

horizontal wavelength 59km

vertical wavelength 20km

period 16mins

omega = N/2

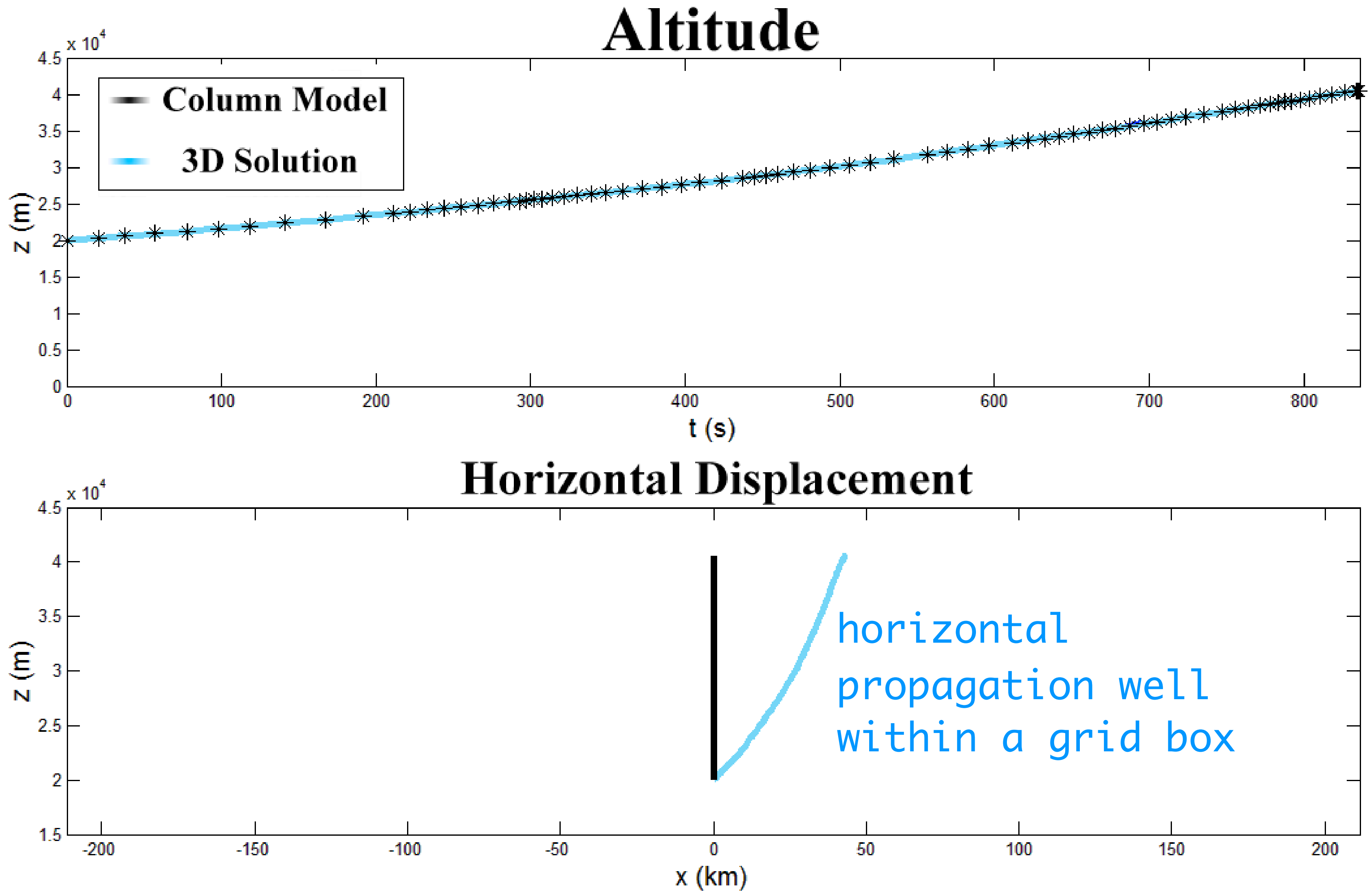

For topographic waves the 3d effects are slight, tested with GCM.

Strong effects require near-inertial waves

The complete ocean circulation, abridged

Schmitz 1996

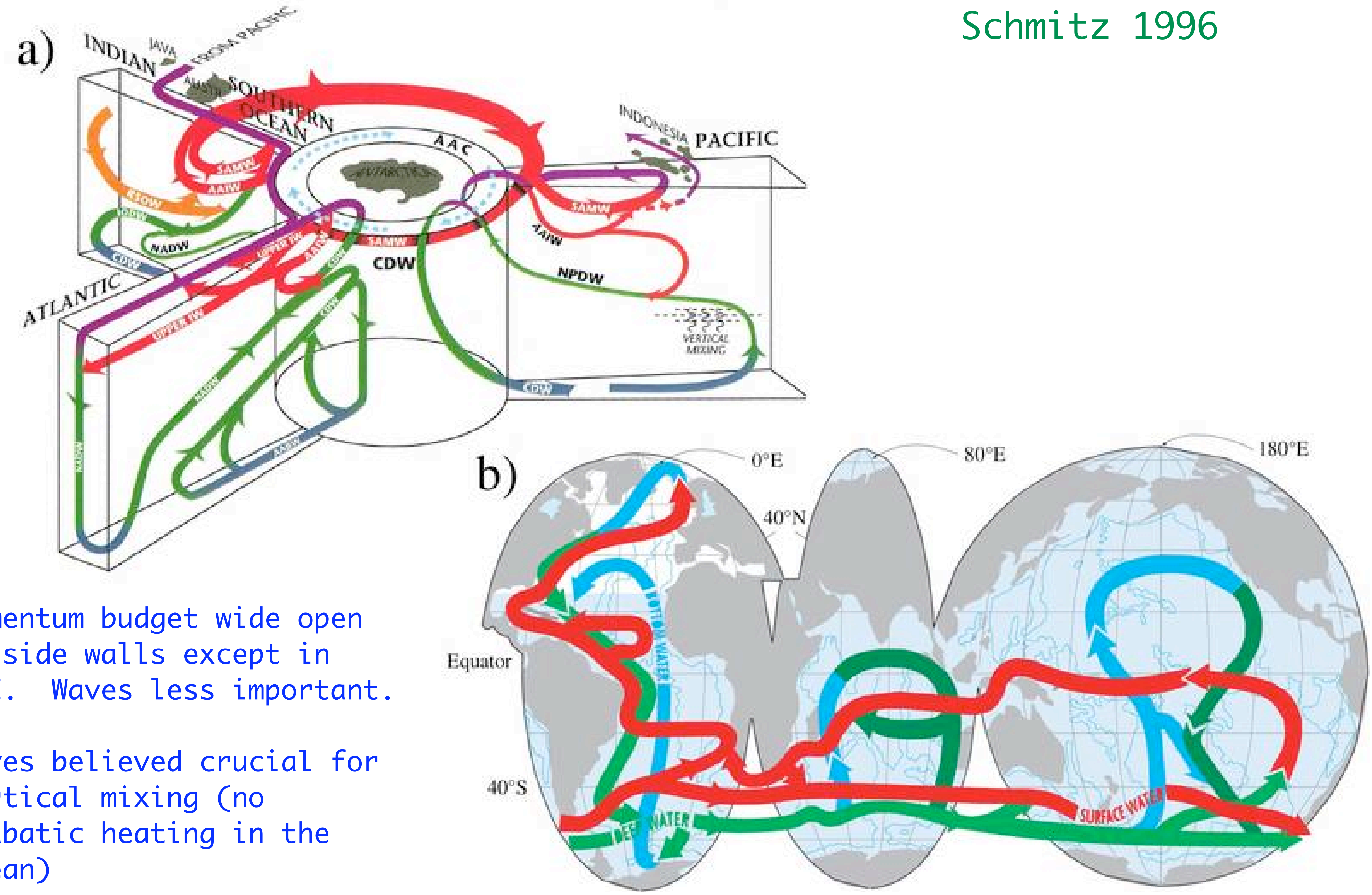

Momentum budget wide open by side walls except in ACC. Waves less important.

Waves believed crucial for vertical mixing (no diabatic heating in the ocean)

Wave-induced diffusivity in the deep ocean

Large-scale overturning circulation advects particles in the meridional plane

Density surfaces should overturn in the meridional plane

Apparently, this does not happen at the right rate and therefore there must be density diffusion ("diapycnal diffusion") of sufficient magnitude

Small-scale gravity waves are believed to play a significant role here: wave-breaking induces mixing and diffusion

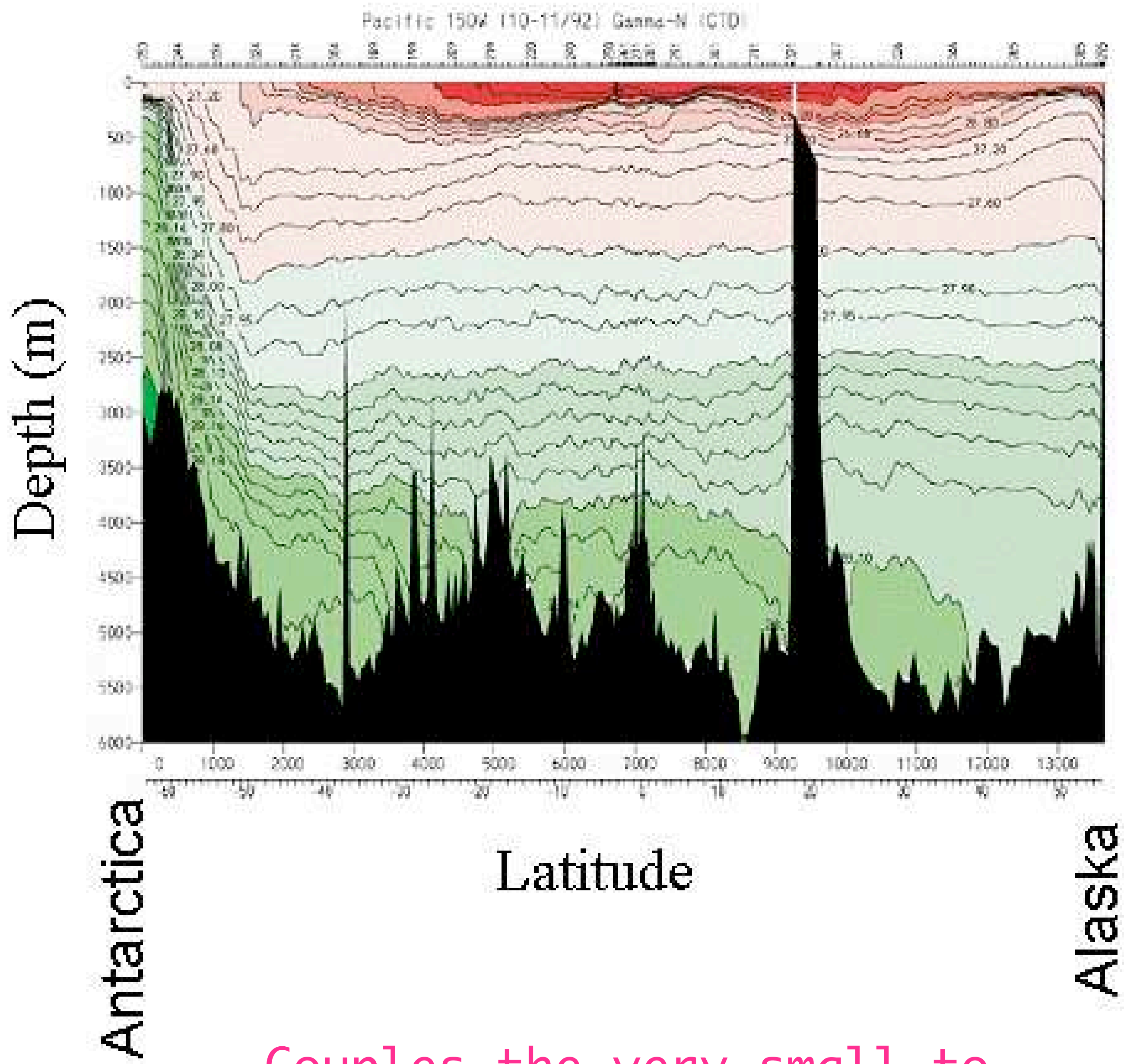

Couples the very small to the very large

Microstructure measurements

Polzin et al. 1997
The plot that launched a 1000 ships

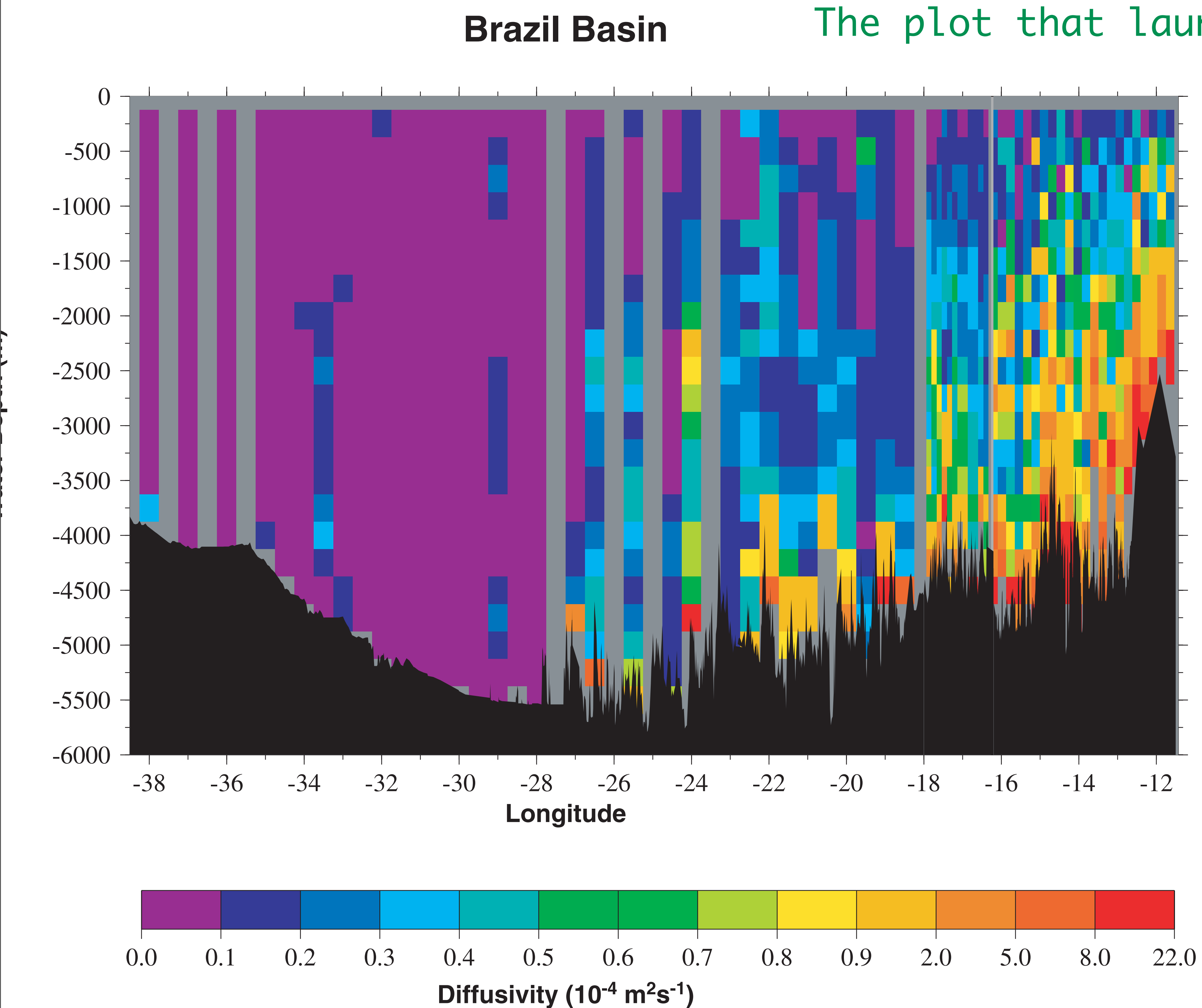

Clear evidence of enhanced turbulence above rough topography

What are internal tides and why do we care?

Internal tides are internal waves generated by the flow of the barotropic tide over the undulating sea-floor

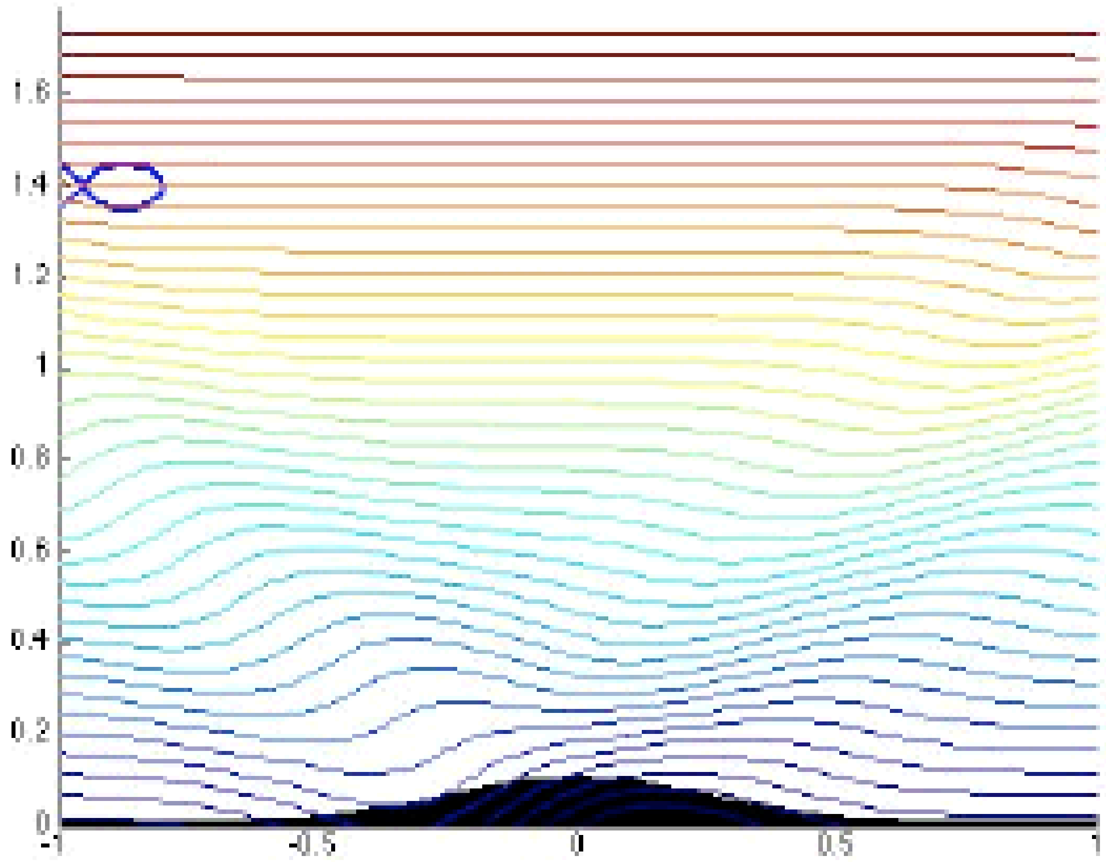

Mathematical model with ocean at rest, bottom topography moving back and forth with barotropic tidal frequency and excursion amplitude 100-200 metres

Dominant internal tides at tidal frequency
Sub-dominant modes at higher harmonics

Internal tide

Barotropic tide (eg M2) rubs over undulating sea-floor topography
Internal waves are generated: “internal tides”
Breaking and dissipation of unstable internal tides provides deep-ocean mixing
Mixing efficiency contingent on spatial distribution of mixing: boundary vs interior

Subtle linear problem in general due to time-dependent Doppler shifting

Easy for small or large tidal excursion parameter

$$\frac{U_0 k}{\omega_0} \ll 1$$

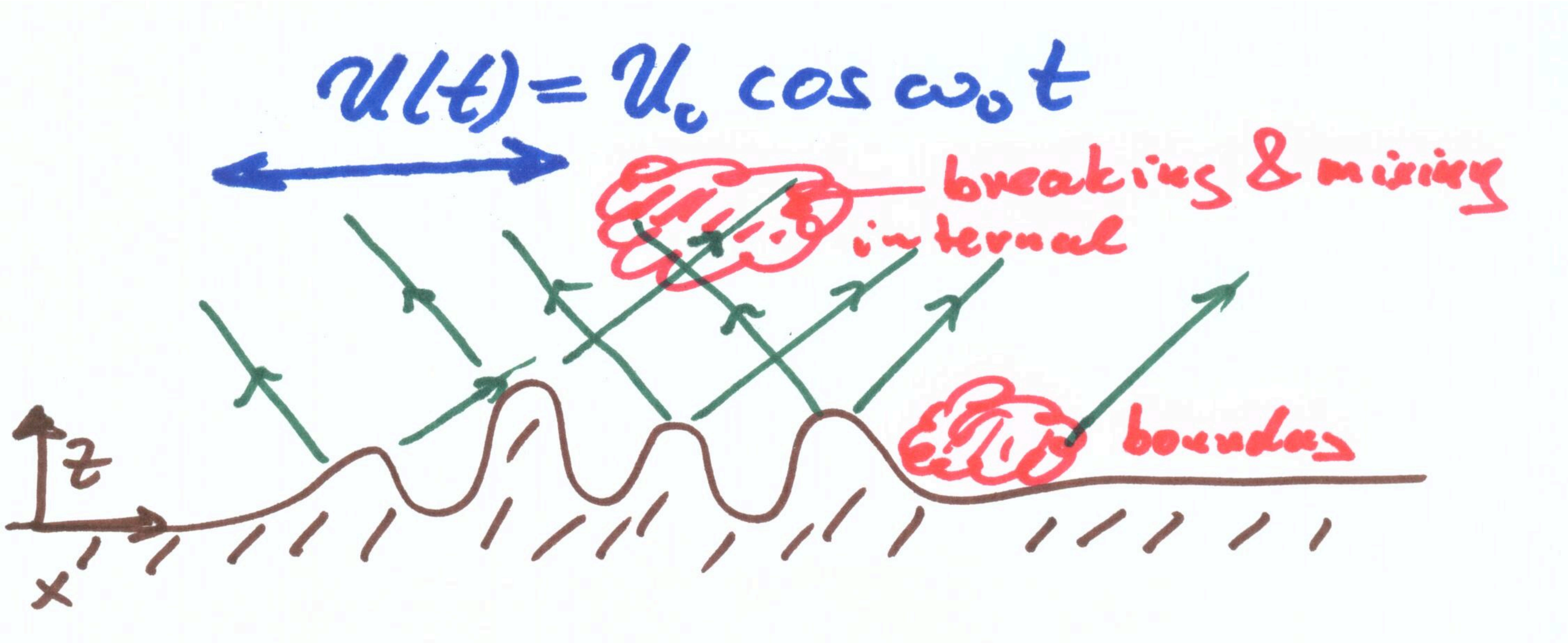

Typically all studies linear, no downslope windstorms knowledge used...

Three-dimensional internal tide

Muller & Bühler JFM 2007

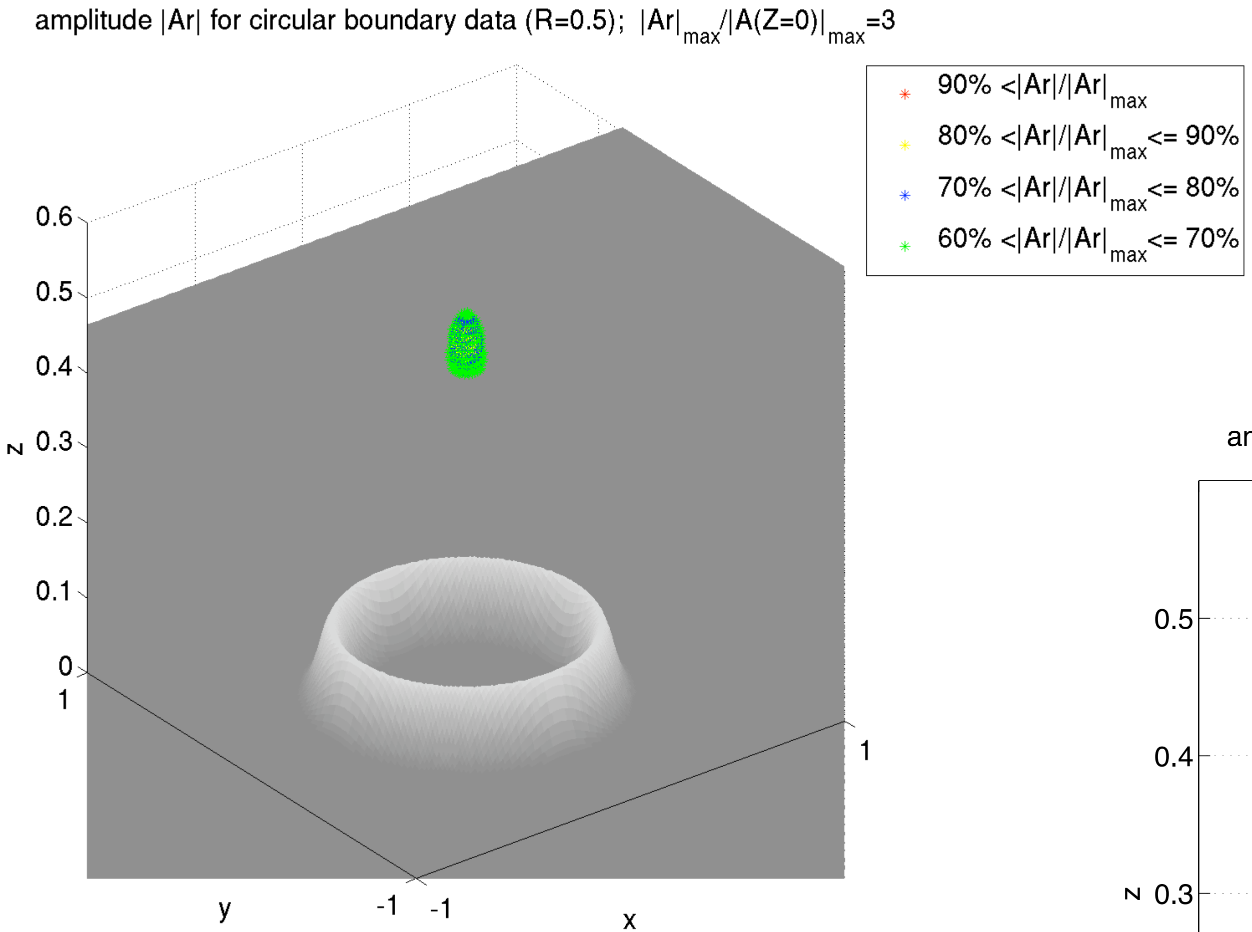

Real part
interior of cone
peaked near front-

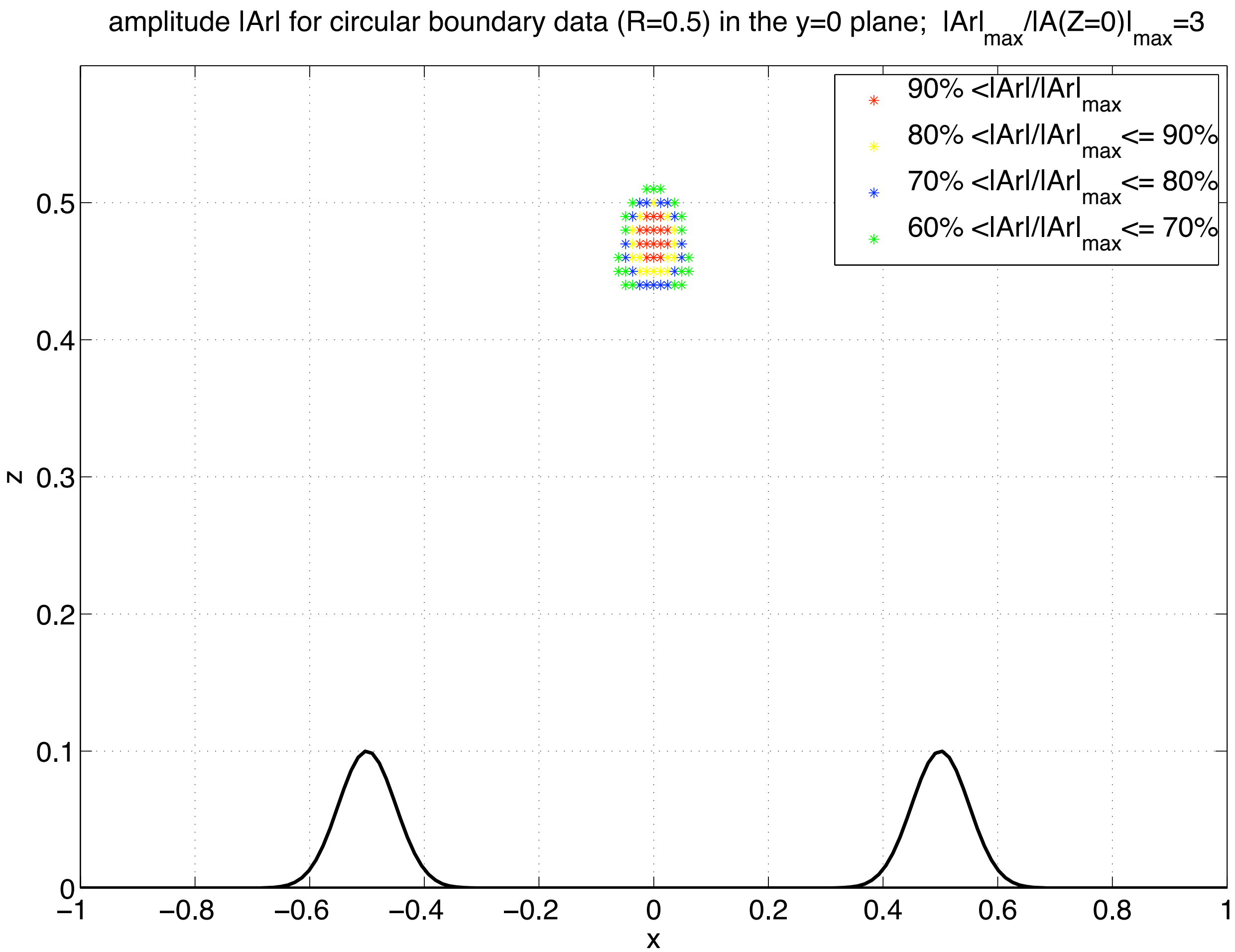

Focuses in a single point

Not generic

Maximal amplification 3 $\propto \sqrt{\frac{R}{\sigma}}$

$R = 0.5 \quad \sigma = 0.05$

3d line focusing

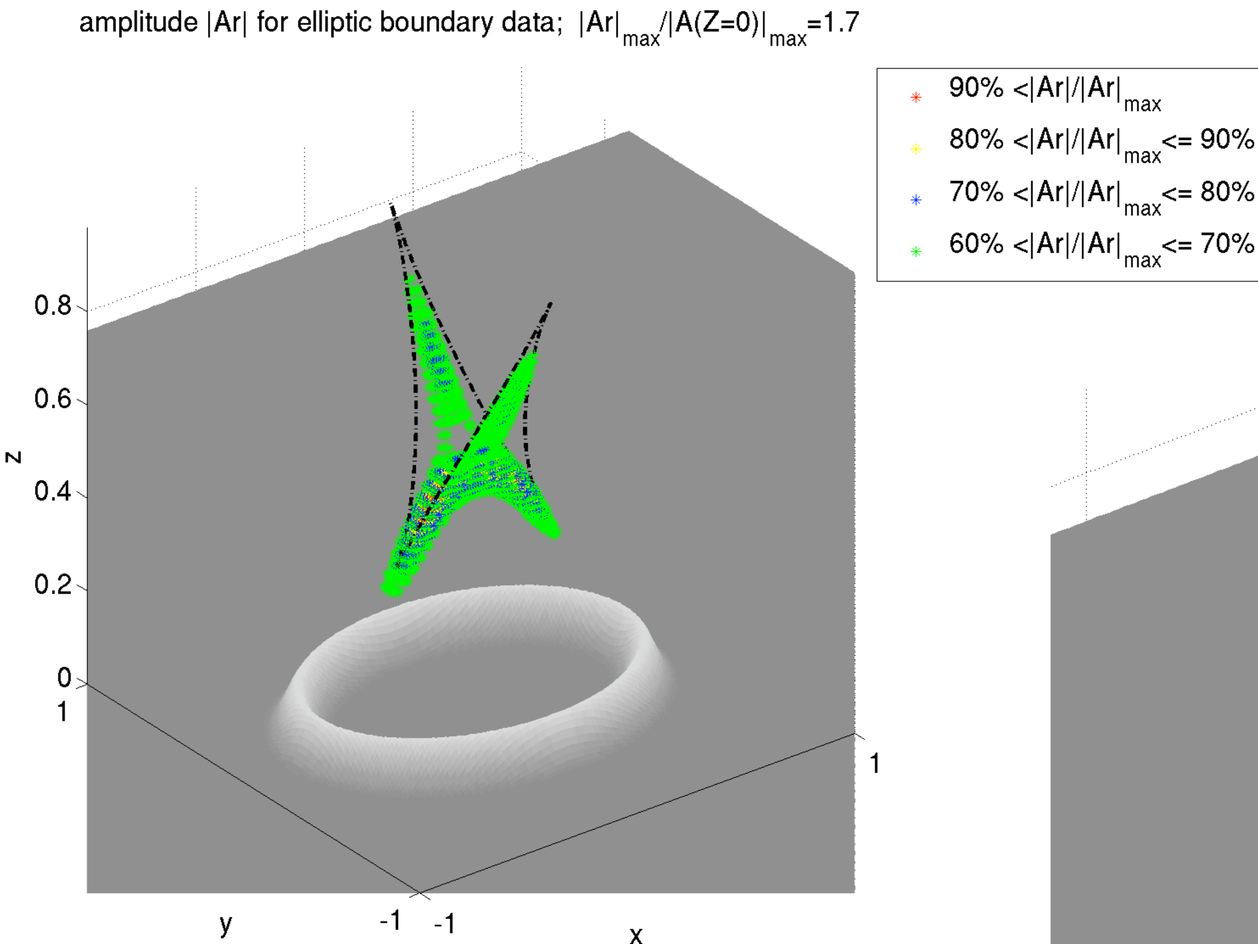

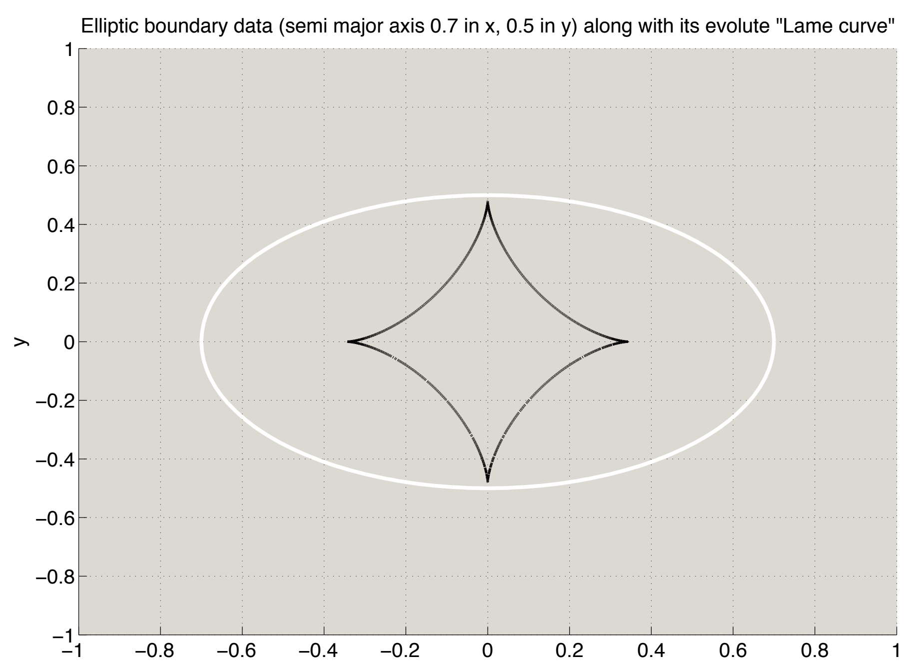

Real part
interior of cone
peaked near front-

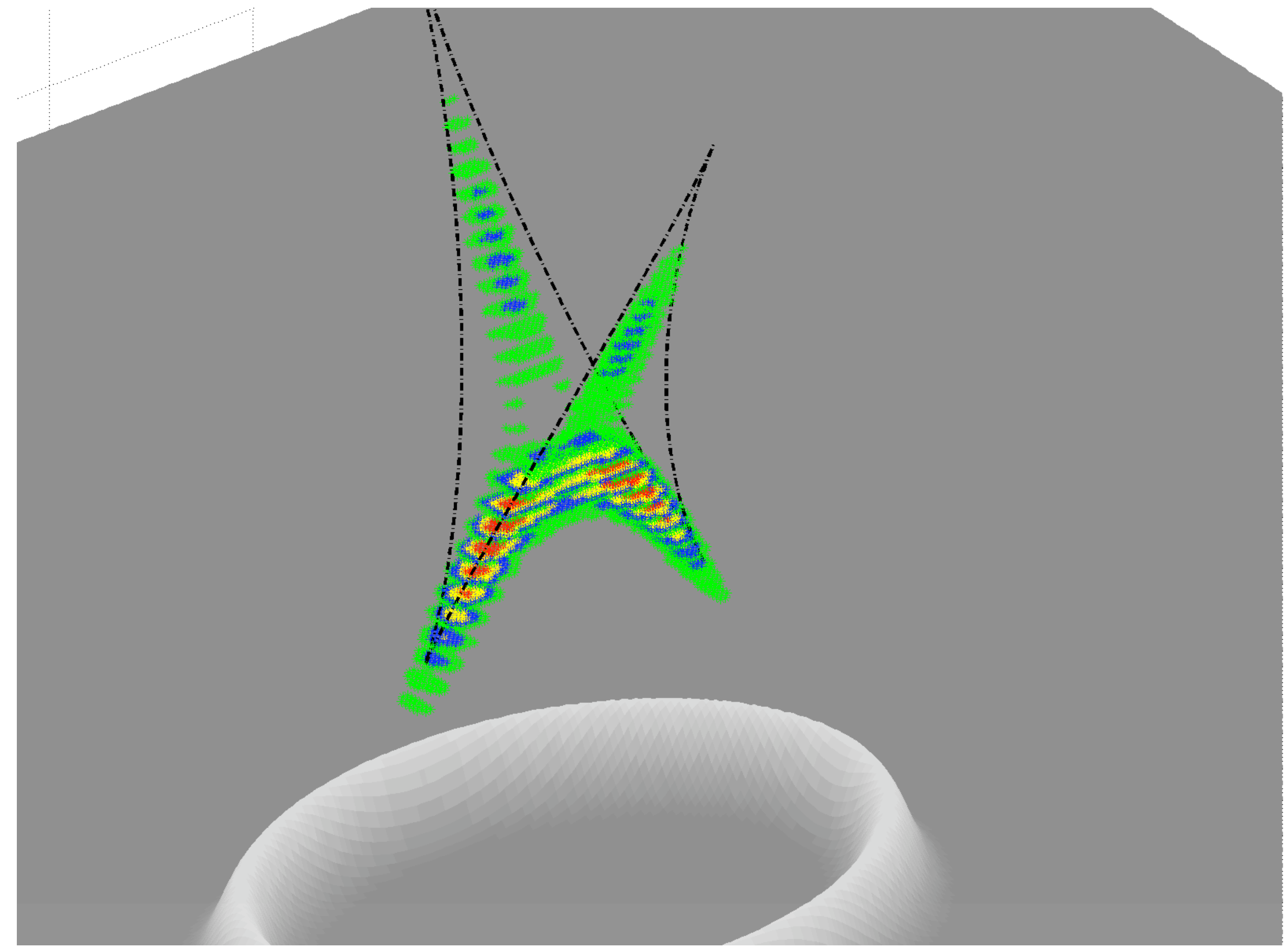

$$a = 0.7 \quad b = 0.5 \quad \sigma = 0.05$$

Saturation of internal tide

Muller & Bühler JPO 2009

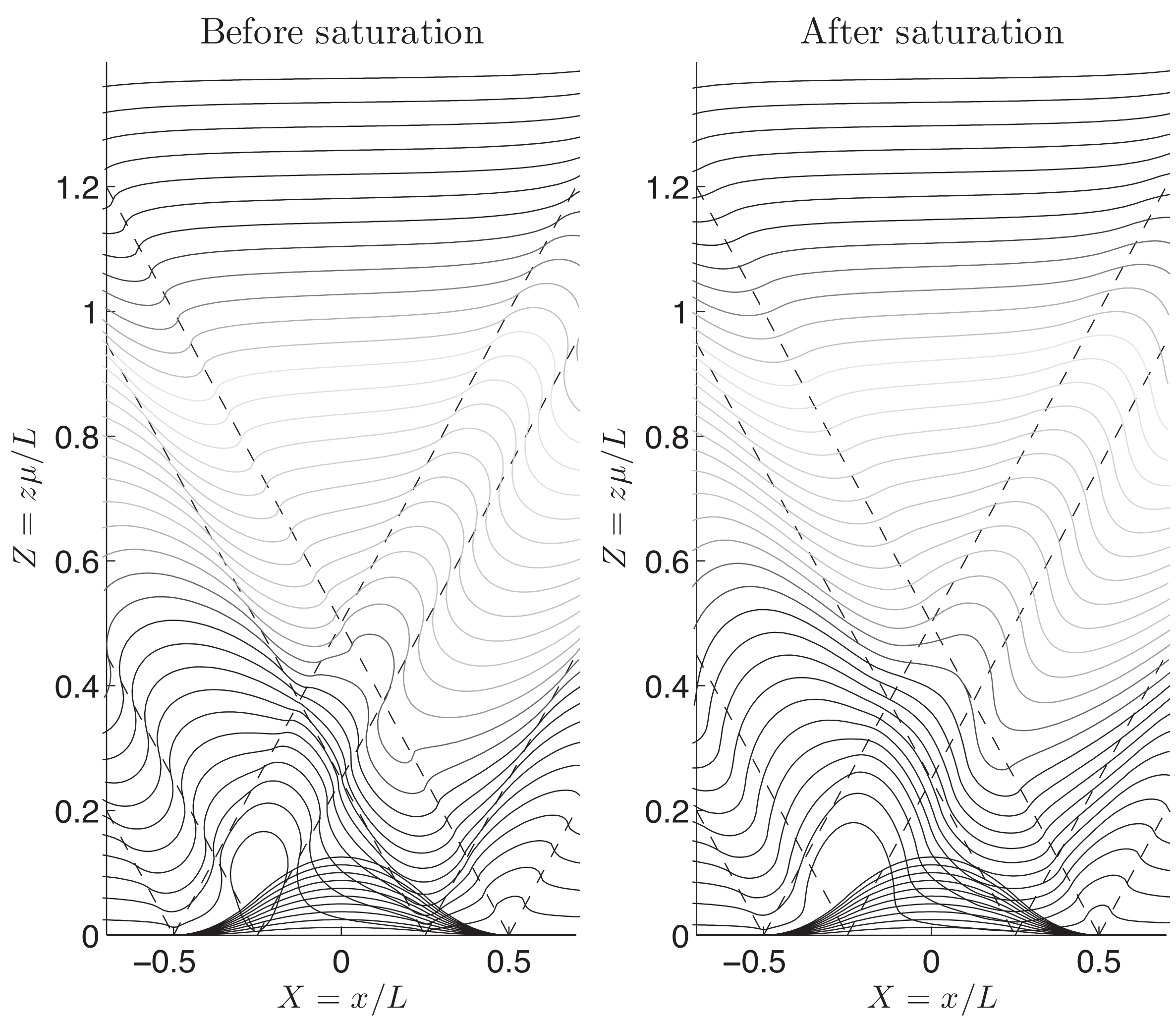

FIG. 2. Buoyancy surfaces with saturation.

Saturation of linear waves using convective instability as criterion.

Works in real space, no plane waves here!

Resultant energy flux convergence can be converted into vertical mixing profile

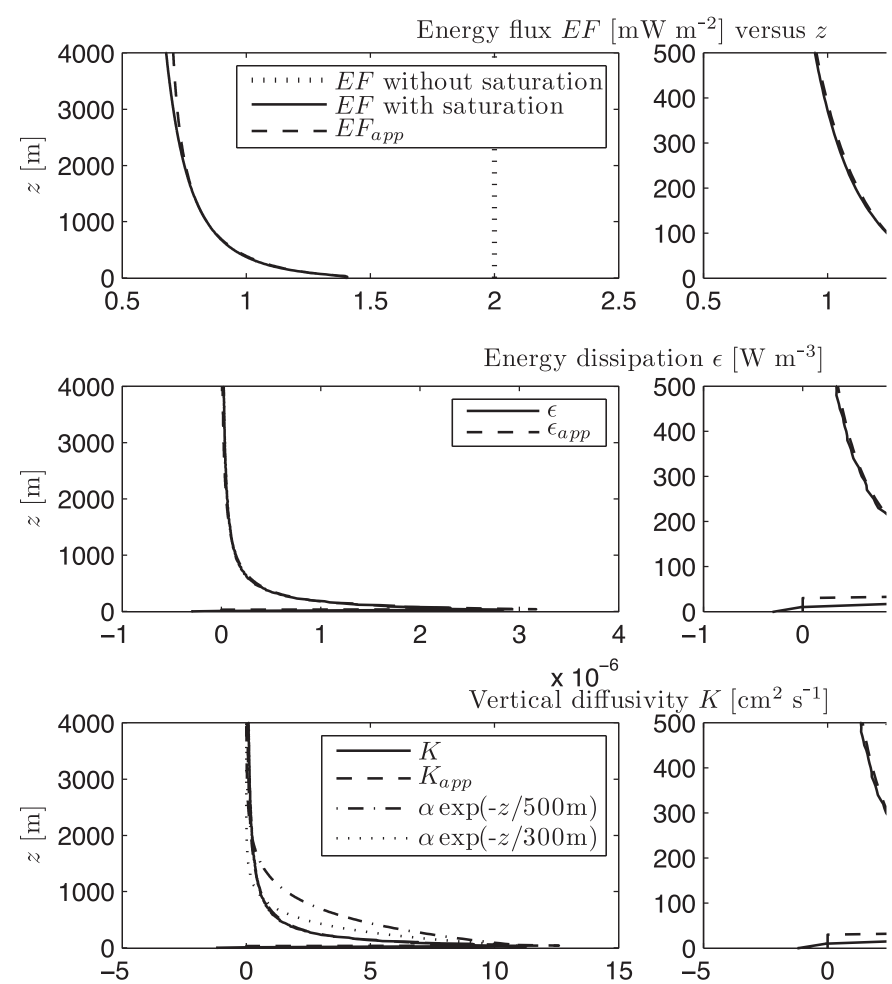

This calculation is repeated for many statistical topography samples and then averaged to obtain the expected diffusivity profile

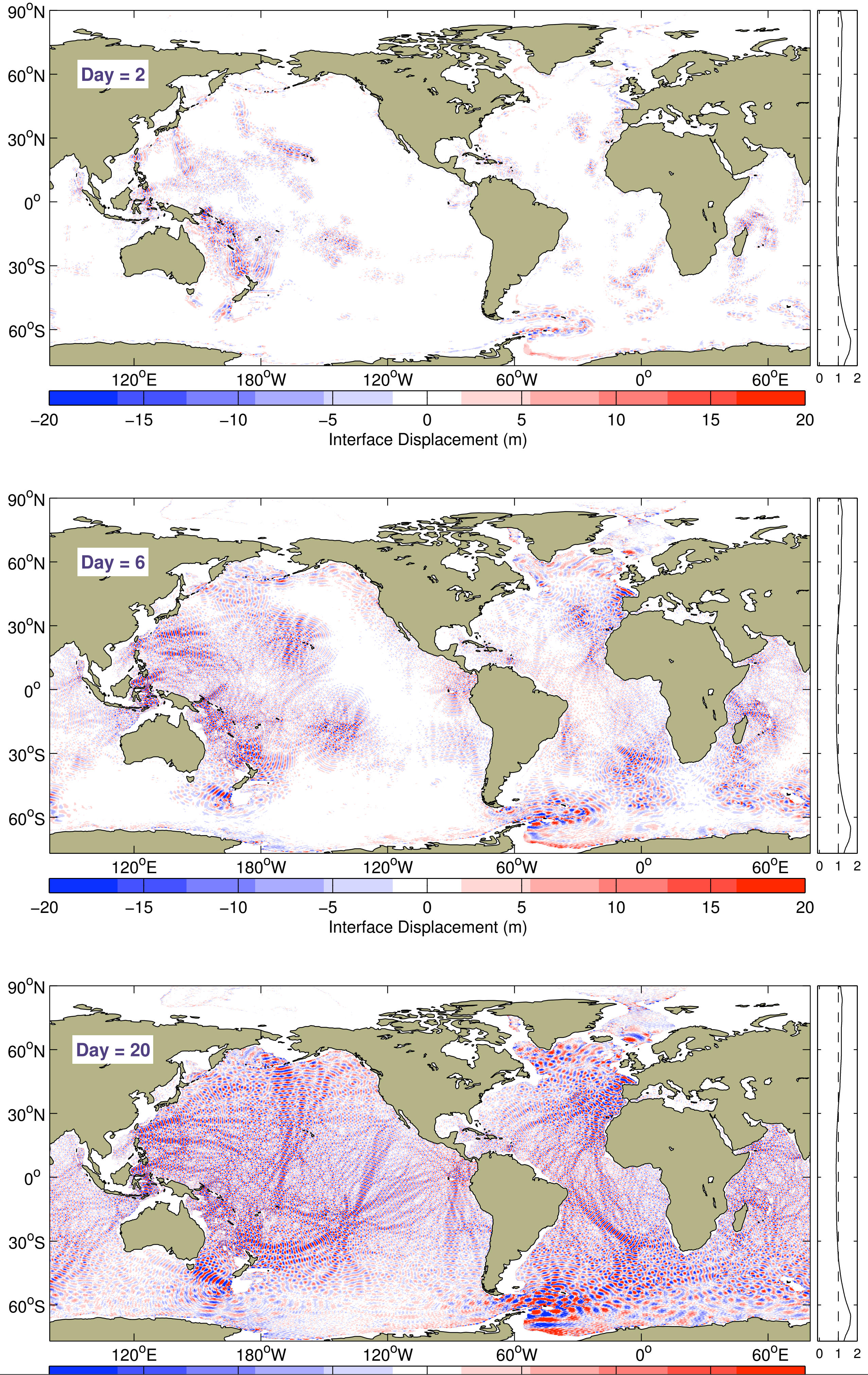

Internal tide spreading through the ocean

Simmons, Hallberg, Arbic 2004 two-layer model

Recent work with
Miranda Holmes-Cerfon:

what limits the propagation of the internal tide?

Scale cascade limits the life time of low mode tides

How far can mode-1 tide propagate?

e.g. M2 tide

$$\psi = \sin\left(\frac{z\pi}{H}\right)\cos(kx - \omega t) \qquad H = 4\mathrm{km}, \quad k = \frac{2\pi}{150\mathrm{km}}$$

This is important for interactions with the mean flow (e.g. the barotropic tide)

Basic fact of wave-mean interaction theory:

the mean flow feels topographic waves not where there are generated but where they are dissipated

Bühler 2009
C.U.P.

"Waves and Mean Flows"

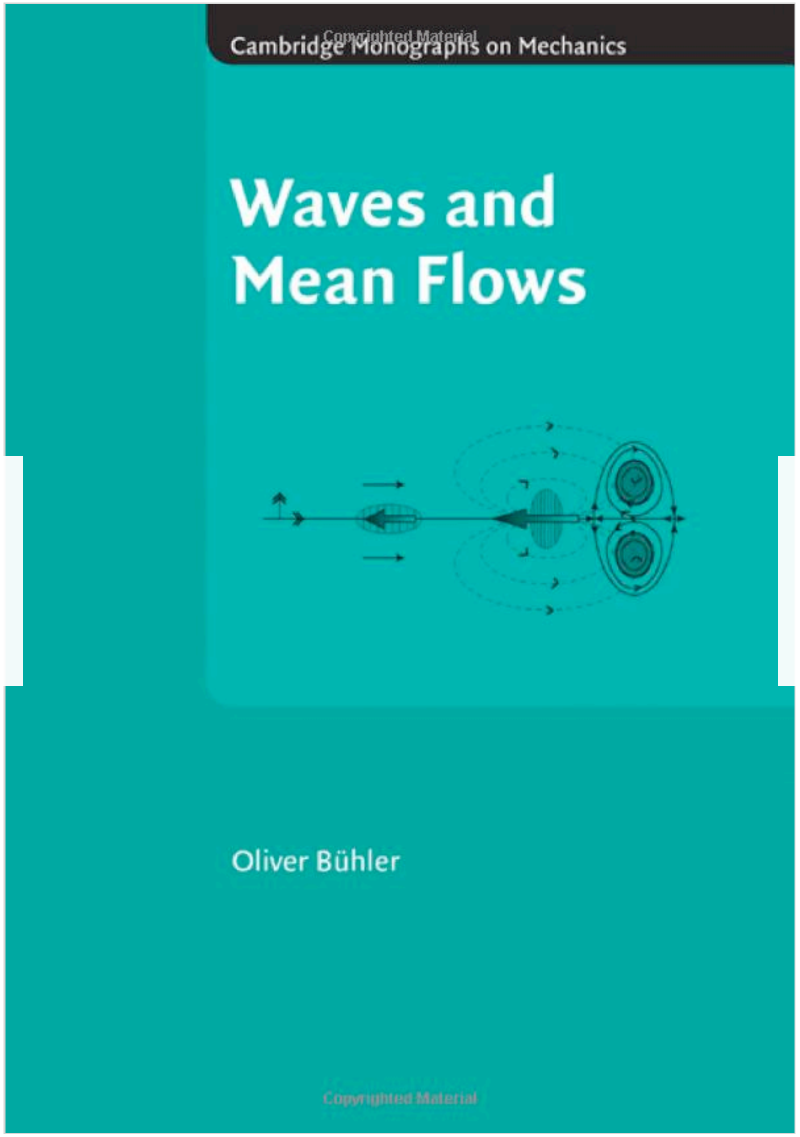

Paper in press, Feb 11

Decay of an internal tide due to random topography in the ocean

By OLIVER BÜHLER †
AND MIRANDA HOLMES–CERFON ‡
Center for Atmosphere Ocean Science at the Courant Institute of Mathematical Sciences
New York University, New York, NY 10012, USA

(Received 5 February 2011)

Problem set-up, 2d

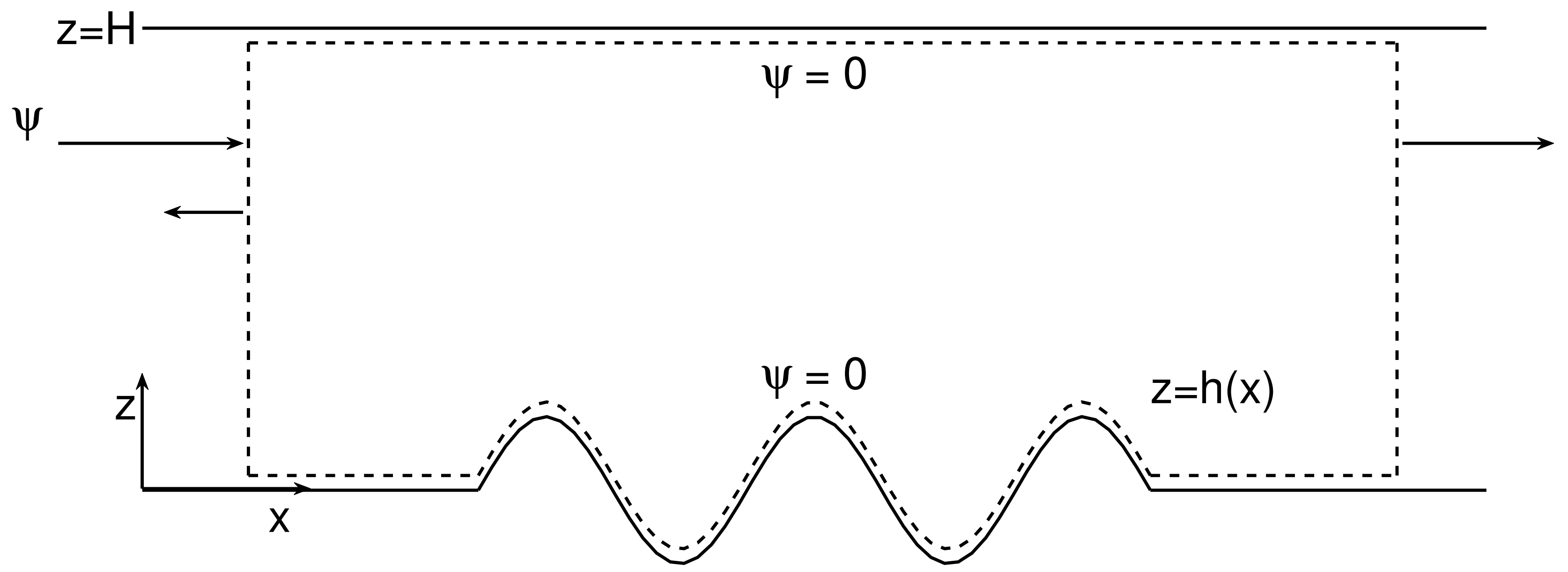

Problem

- Random topography $h(x)$ (Gaussian)
- Linear internal wave equation

$$(N^2 + \partial_{tt})\partial_{xx}\psi + (\partial_{tt} + f^2)\partial_{zz}\psi = 0$$

$\psi =$ streamfunction, s.t. $u = \partial_z\psi$, $w = -\partial_x\psi$.

Boundary conditions

rotation included

- Top, bottom: $\psi = 0$ at $z = H, z = h(x)$
- Prescribed incoming waves at $x = -\infty$
- Radiation condition: no other incoming waves at $x = \pm\infty$

Spatial mode structure

Look at fixed frequency ω: $\psi(x, z, t) = \Psi(x, z)e^{-i\omega t}$.

$$z = \frac{H}{\pi}z', \quad x = \frac{1}{\mu}\frac{H}{\pi}x', \qquad \mu = \sqrt{\frac{\omega^2 - f^2}{N^2 - \omega^2}}$$

Slope of wave rays, ~ 0.2 for tidal modes.

Non-dimensional equation

$$\Psi_{xx} - \Psi_{zz} = 0$$

Form of solution

$$\Psi = f(\xi) + g(\eta),$$

$$\xi = x + z - \pi, \quad \eta = x - z - \pi.$$

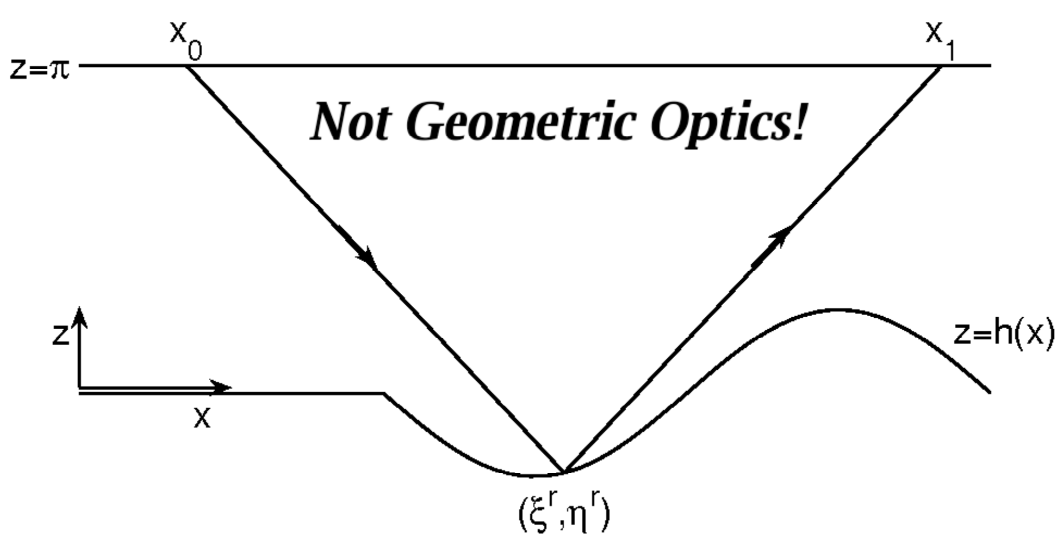

- b.c. $\Psi = 0$ at $z = \pi \quad \Rightarrow$ $g(\xi) = -f(\xi)$
- Remains to determine:
  1. function $f(\xi)$
  2. characteristic map $x_0 \to x_1$

Solution along characteristics

Solution

$$\Psi = f(\xi) - f(\eta), \qquad \xi = x + z - \pi, \quad \eta = x - z - \pi.$$

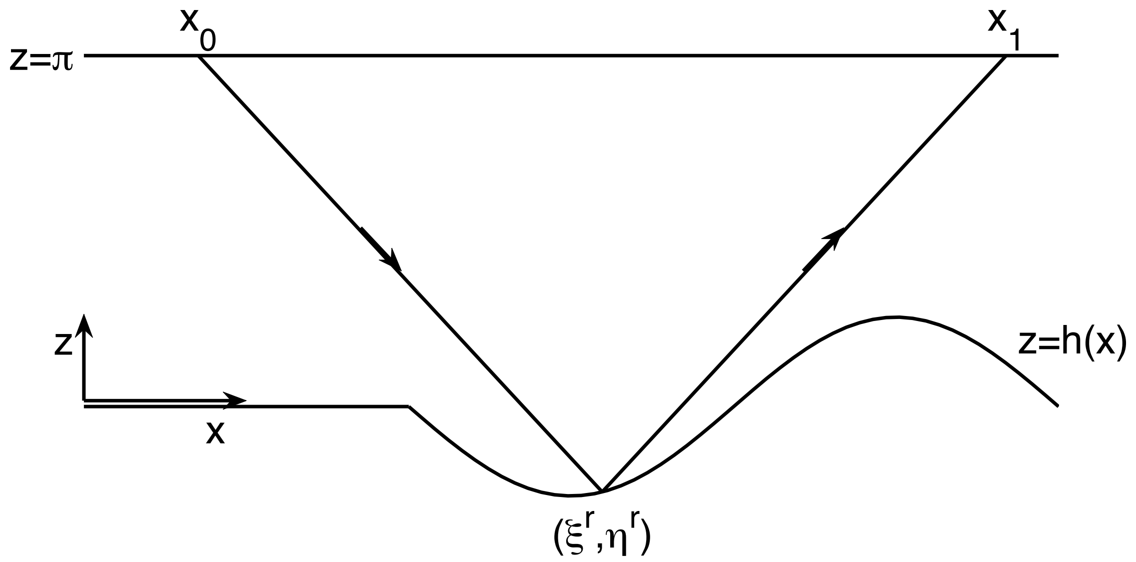

Ill-posed problem for the spatial structure of time-periodic internal waves in a bounded domain

First pointed out by Sobolev 1930s in connection with research into rotating fuel tanks

Wunsch 1960s

Maas et al 1990s

- ξ is constant on incoming ray
- $f(\eta^r) = f(\xi^r) = f(\xi_0)$
- η is constant on reflected ray
- $f(\xi_1) = f(\eta_1) = f(\eta^r) = f(\xi_0)$

$$x_0 = \xi_0, \quad x_1 = \xi_1$$

$$\Rightarrow \boxed{f(x_0) = f(x_1)}$$

Weaving a tangled web

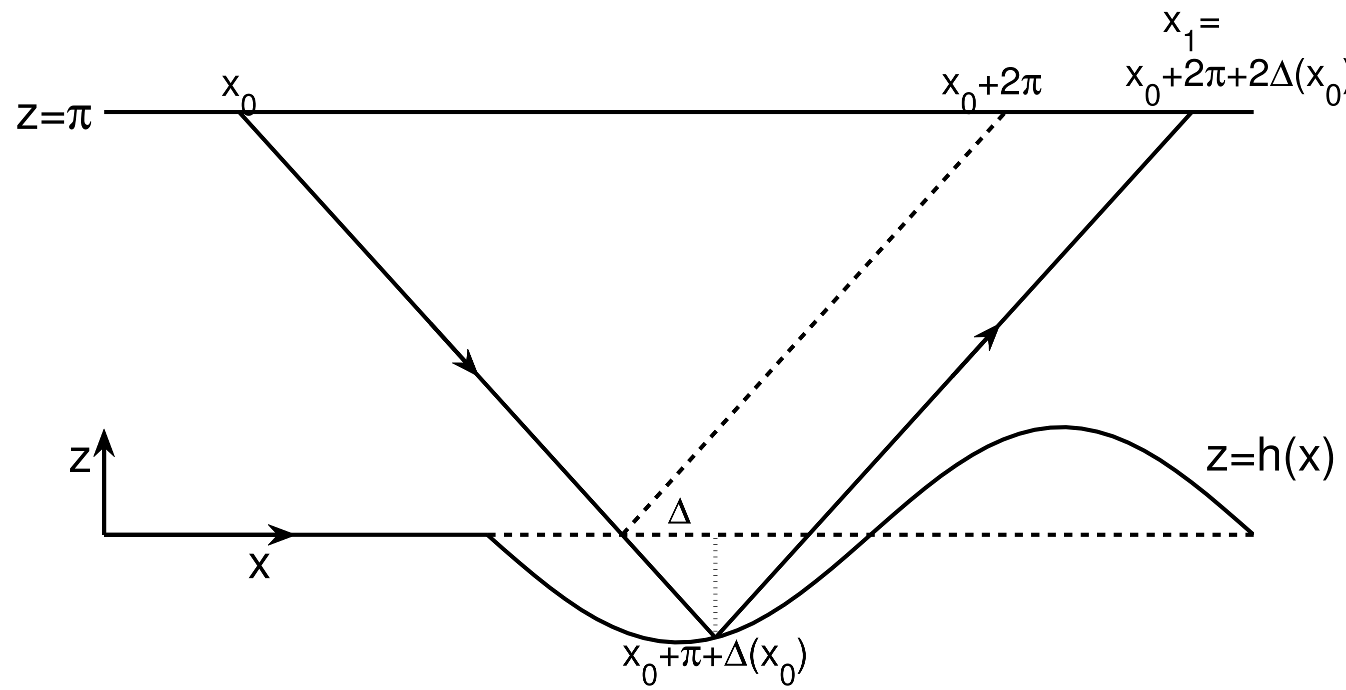

One bounce: $x \to r_1(x) = x + 2\pi + 2\Delta(x)$

Where $\Delta(x)$ solves

$$h(\pi + x + \Delta(x)) + \Delta(x) = 0$$

$$|h| \ll 1 \quad \Longrightarrow \quad \Delta(x) = -h(x+\pi) + O(|h|^2)$$

$$\Longrightarrow \quad \Delta(x) \stackrel{d}{=} -h(x)$$

Many bounces: $r_{n+1}(x) = r_n(x) + 2\Delta_n(r_n(x))$

Transmission + Reflection

Map $\quad r(x) : [0, 2\pi] \to [0, 2\pi] + L$

$$f(r(x)) = f(x),$$
$$f(r^{-1}(x)) = f(x)$$

"Naive" solution

$f_i(\xi)=a_1 e^{i\xi}$ $\longrightarrow$

$f_n(\xi)=\Sigma_{k=-\infty}^{\infty} a_k^{(n)} e^{ik\xi}$ $\longrightarrow$

$\longleftarrow$

True solution

$f_i(\xi)=a_1 e^{i\xi}$ $\longrightarrow$

$f_t(\xi)=\Sigma_{k=1}^{\infty} a_k^{+} e^{ik\xi}$ $\longrightarrow$

$\longleftarrow$

$f_r(\xi)=\Sigma_{k=0}^{\infty} a_k^{-} e^{-ik\xi}$

Periodic topography non-resonant

Topography wavenumber = 1.5

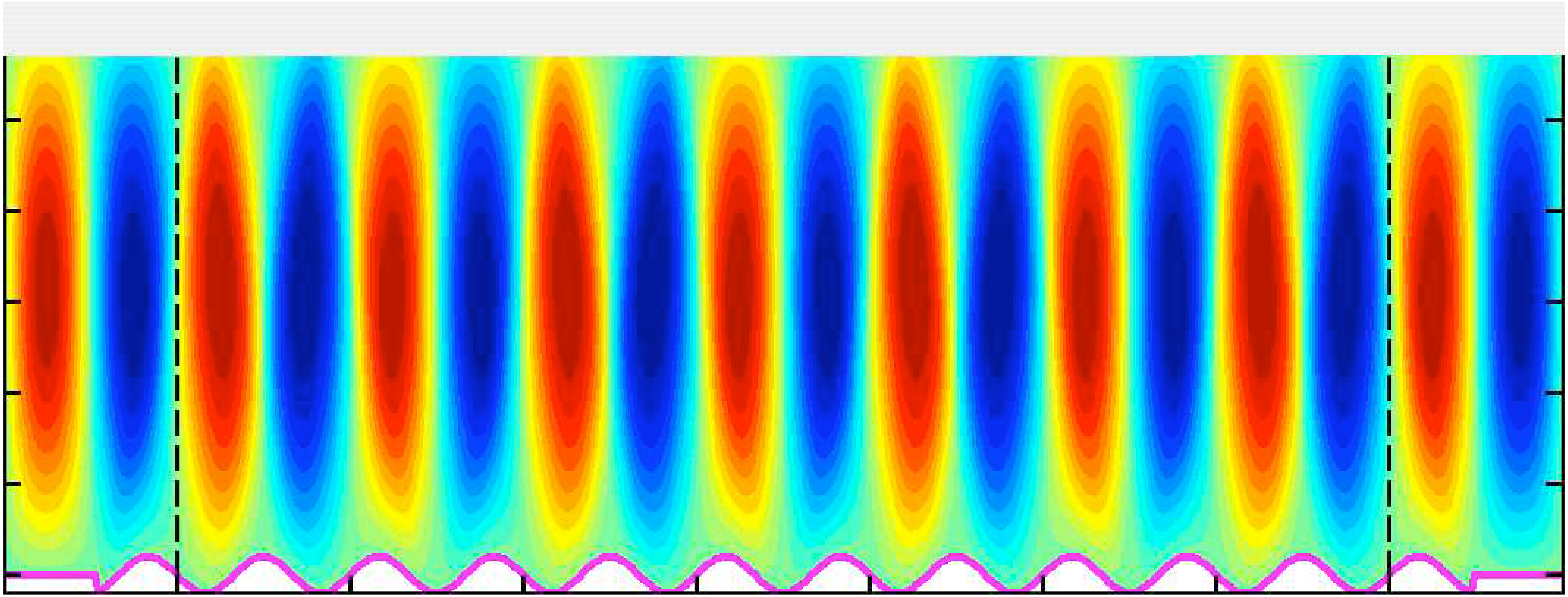

Periodic topography resonant

Topography wavenumber = 1.0

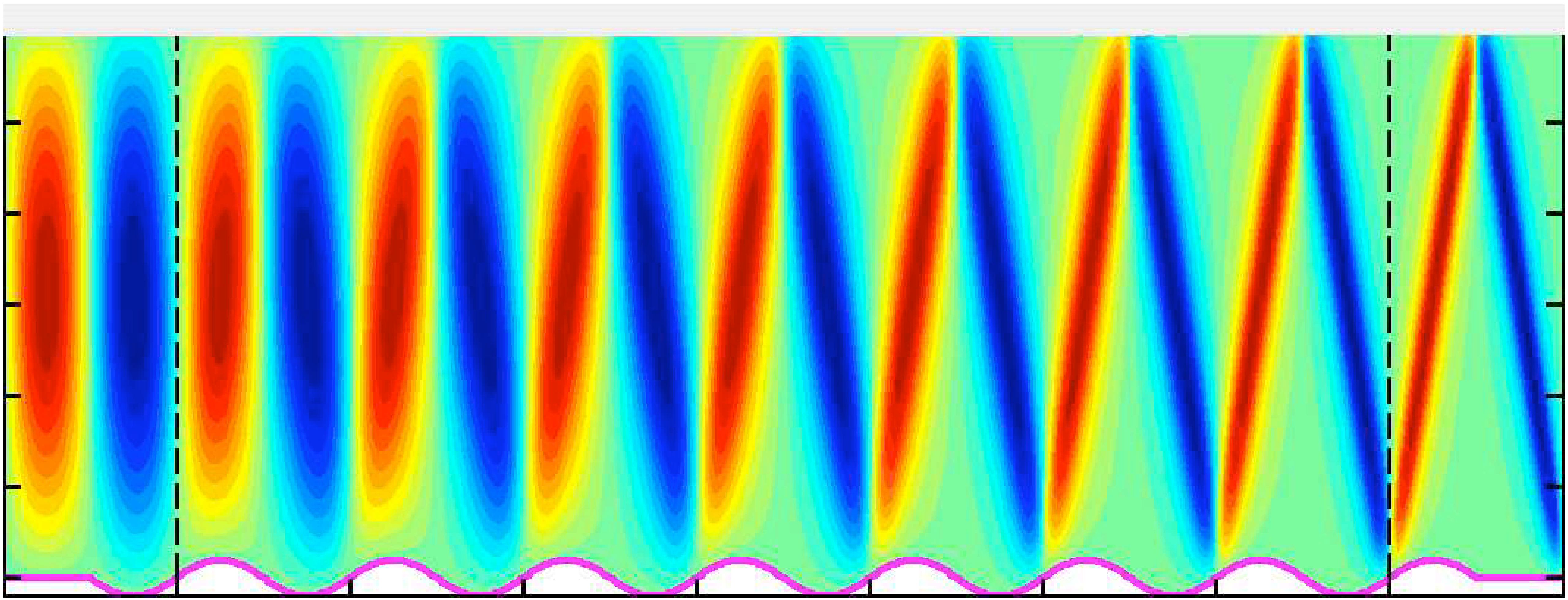

Periodic topography resonant

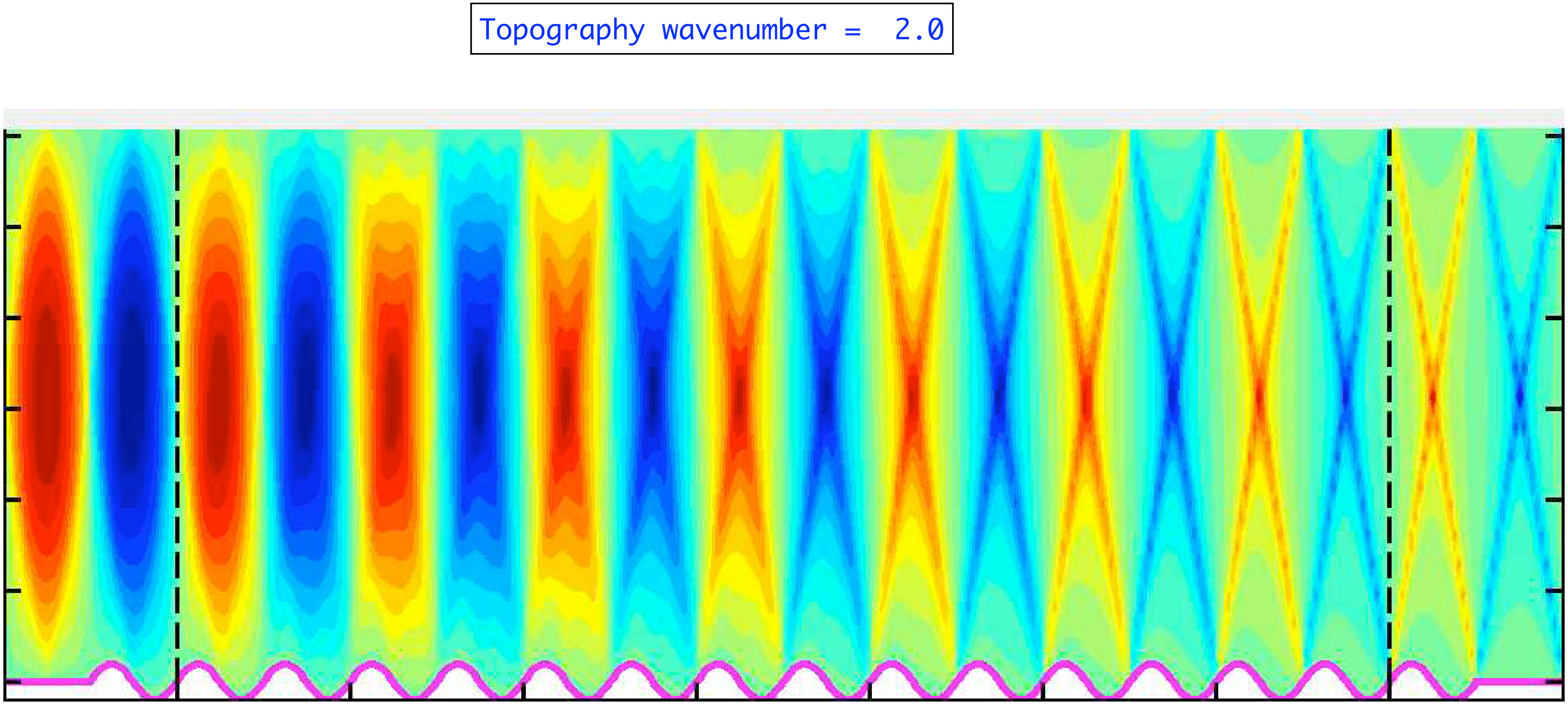

Mode-1 periodic topography

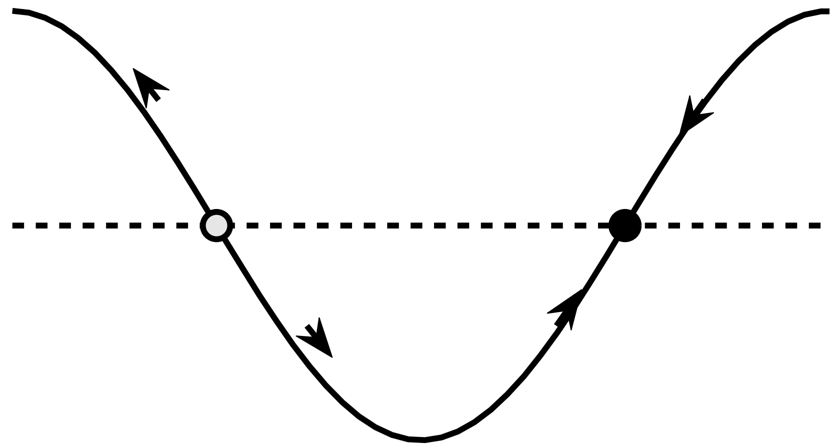

GFD project 2009
Erinna Chen, UCSC
Neil Balmforth, UBC
OB

$$h(x) = \tfrac{1}{2}\cos x$$

$$r_{n+1}(x) \;=\; r_n(x) + 2\Delta(r_n(x)) \;\approx\; r_n(x) - 2h(r_n(x))$$

Continuous approximation $\quad n \rightarrow t$

Footpoint finds the stable fixed point

$$\dot{x} = F(x), \qquad F(x) = -2h(x)$$

Focusing

Initial streamfunction

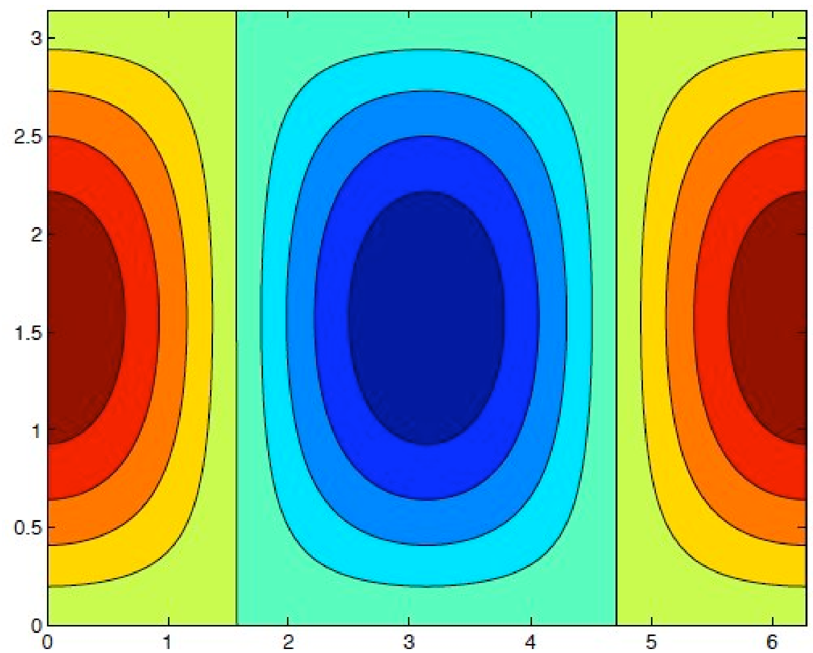

25 bounces

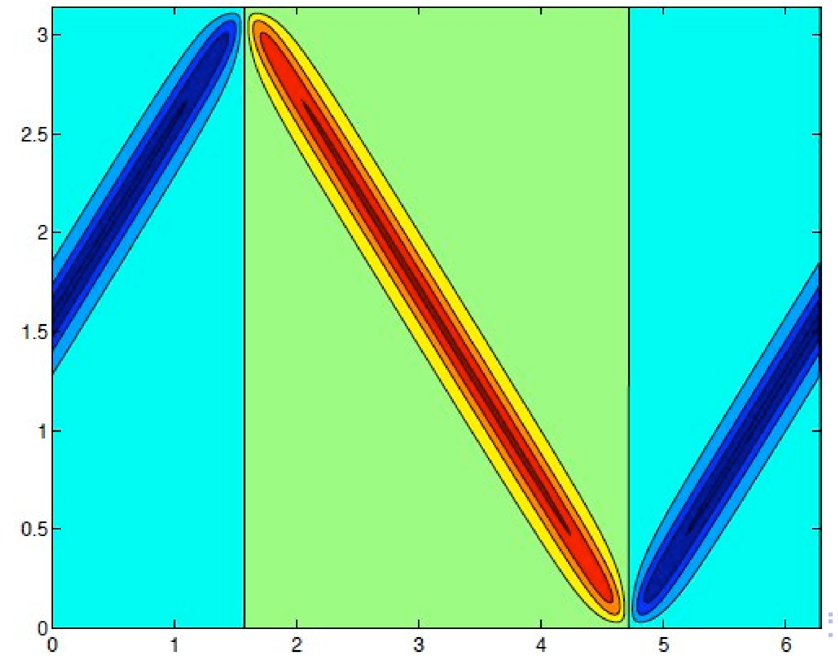

Does this focusing persist for irregular topography?

Encore une fois avec la topographie randomique

Solve problem for random, Gaussian topography:

$$h(x) = \sum_k A_k \cos(kx) + B_k \sin(kx), \quad A_k, B_k \sim \mathcal{N}(0, \hat{C}_k),$$

Covariance function $\mathbb{E}h(y)h(y+x) = C(x) = \sum_k \hat{C}_k \cos(kx)$

Look at:

- properties of map $r(x)$
- scattering rate of incoming mode 1 wave
  - reflected + transmitted energy fluxes: scaling laws depending on topography

Smooth random topography

$$C(x) = \mathbb{E}h(x)h(0) = \sigma^2 e^{-\frac{1}{2}(\frac{x}{\alpha})^2}, \qquad \sigma = 0.1,\ \alpha = 0.25$$

One bounce

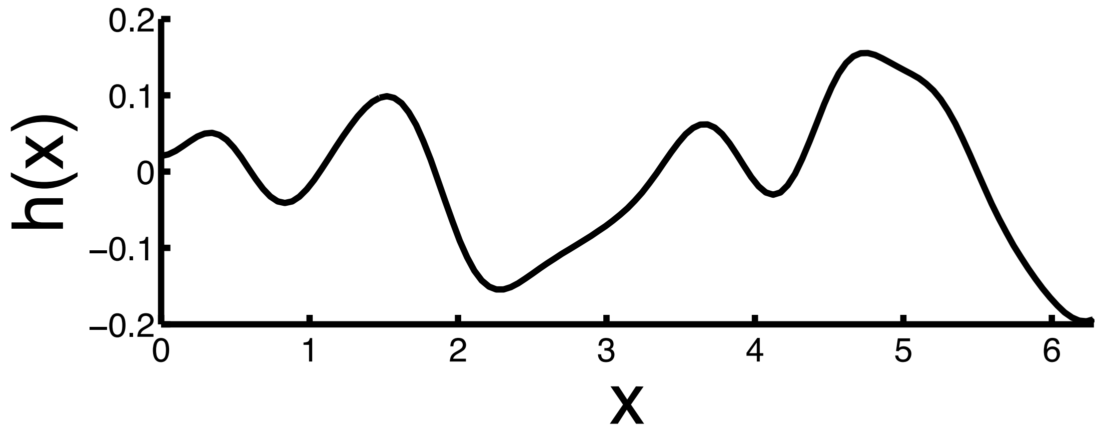

7 bounces

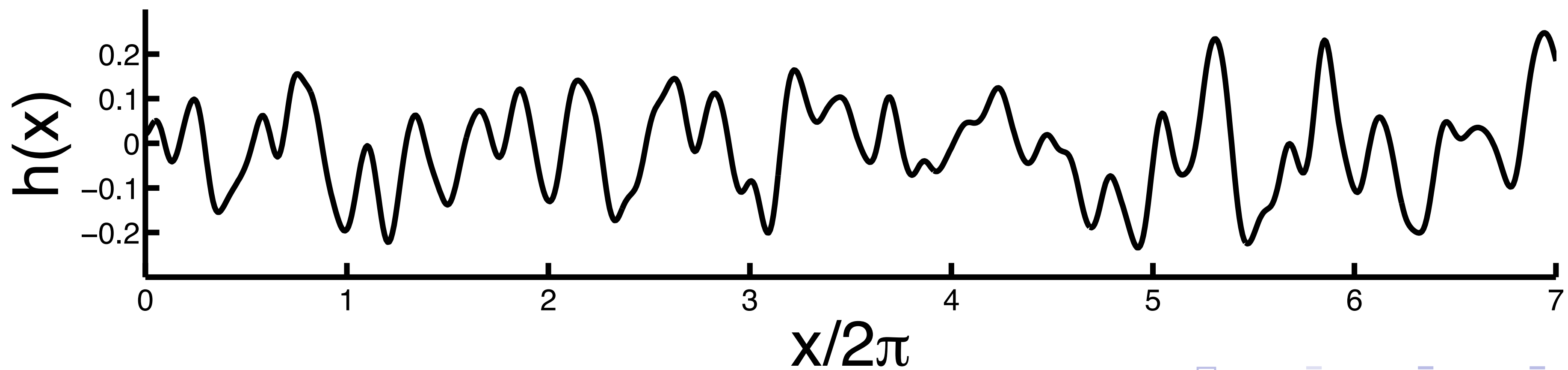

Every collection of h(x_1), h(x_2), h(x_n) is governed by an n-variate Gaussian distribution

Random topography

Gaussian random topography with Gaussian spectrum

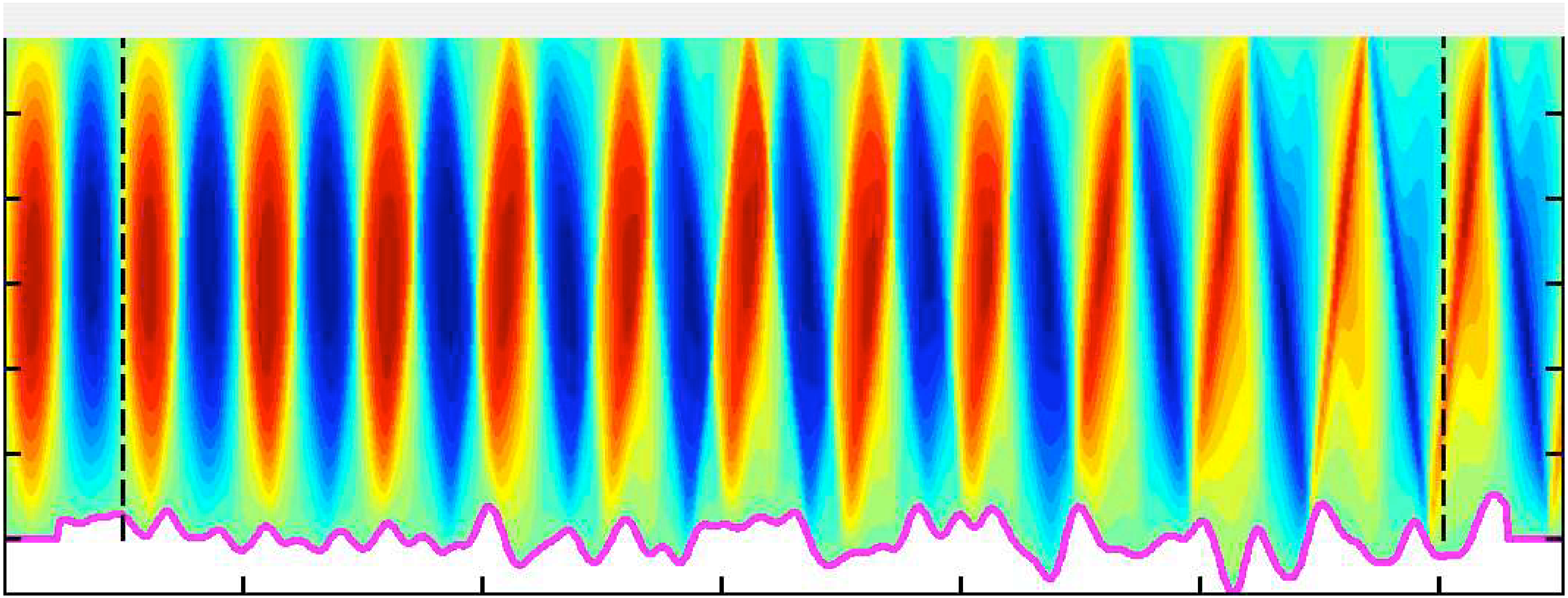

Focusing persists for random topography

$$C(x) = \mathbb{E}h(x)h(0) = \sigma^2 e^{-\frac{1}{2}\left(\frac{x}{\alpha}\right)^2}, \qquad \sigma = 0.1,\ \alpha = 0.25$$

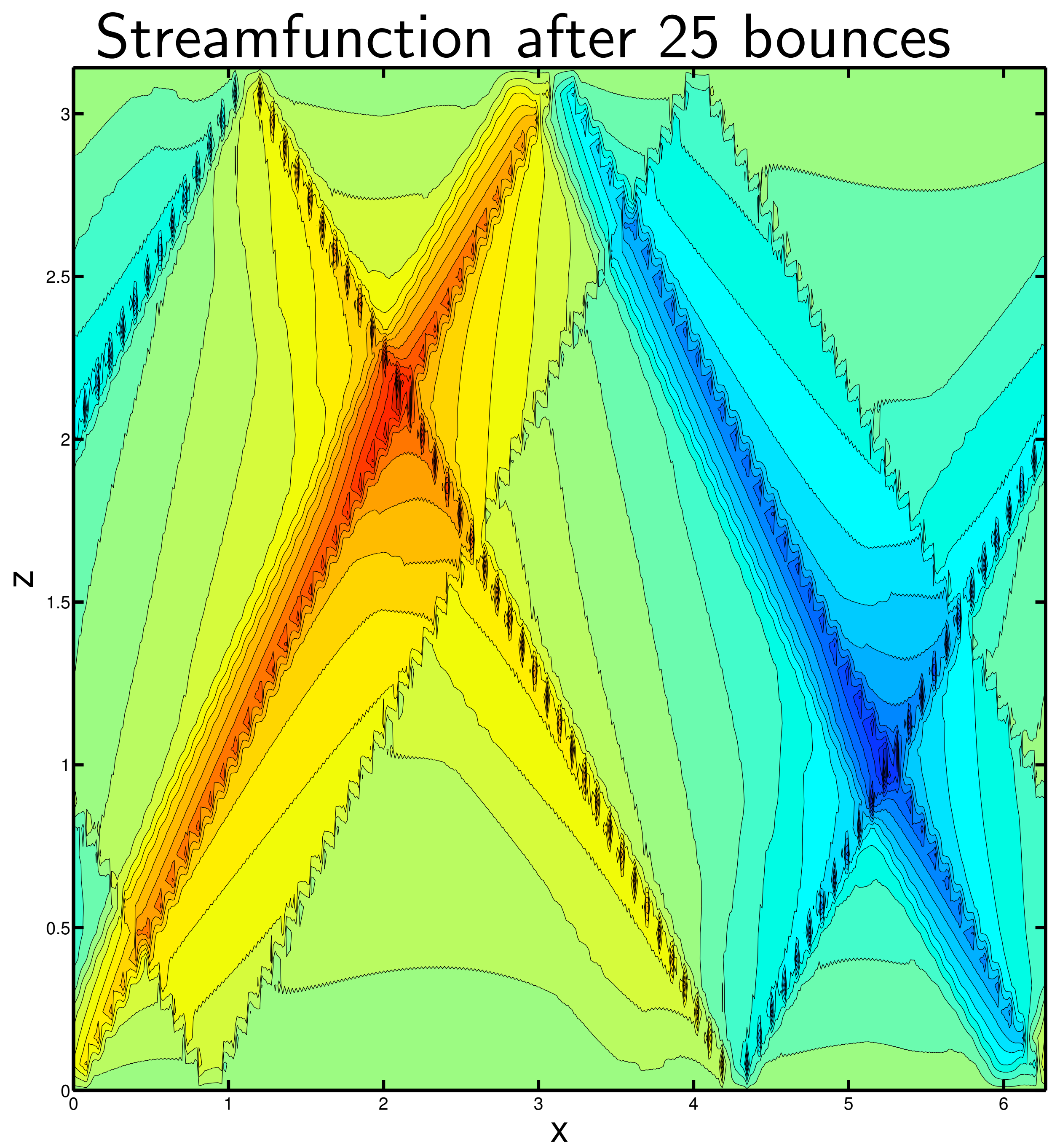

Simple model for pair random walk

$$dX_t^{(1)} = \sum_{k=-\infty}^{\infty} \sqrt{\hat{C}_k}\, e^{ikX_t} dB_t^k$$

$$dX_t^{(2)} = \sum_{k=-\infty}^{\infty} \sqrt{\hat{C}_k}\, e^{ikX_t} dB_t^k$$

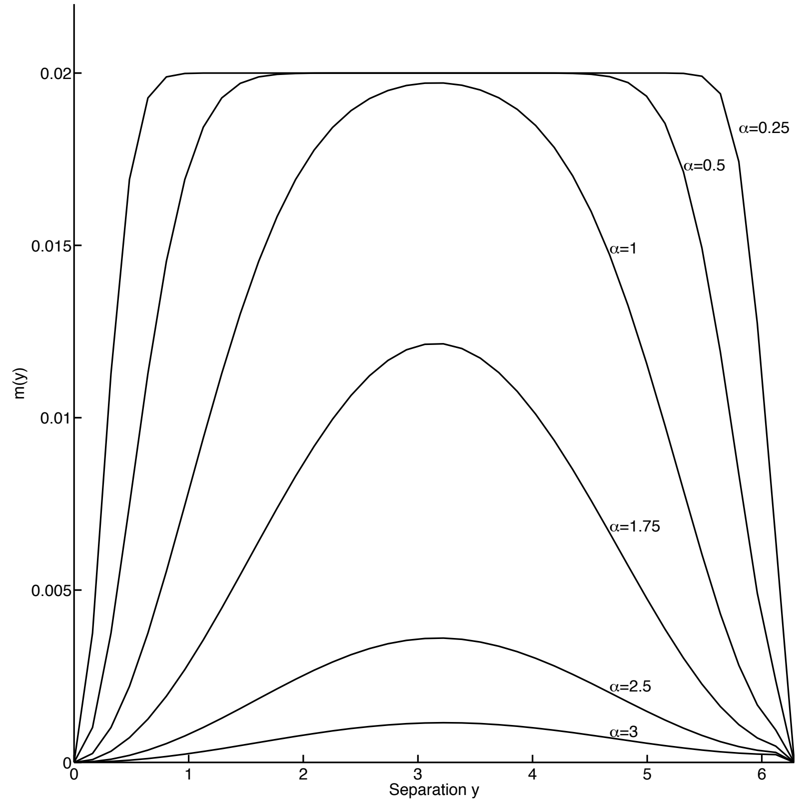

Relative separation $Y_t = X_t^{(1)} - X_t^{(2)}$ solves

$$dY_t = 2\sqrt{C(0) - C(Y_t)}\, dB_t$$

Generic clumping of deterministic walkers in random environment

For small Y:

$$dY_t \approx c_0 Y_t dB_t,$$

Geometric Brownian Motion, which goes to zero almost surely.

Simple model for pair random walk

$$dX_t^{(1)} = \sum_{k=-\infty}^{\infty} \sqrt{\hat{C}_k} e^{ikX_t} dB_t^k$$

$$dX_t^{(2)} = \sum_{k=-\infty}^{\infty} \sqrt{\hat{C}_k} e^{ikX_t} dB_t^k$$

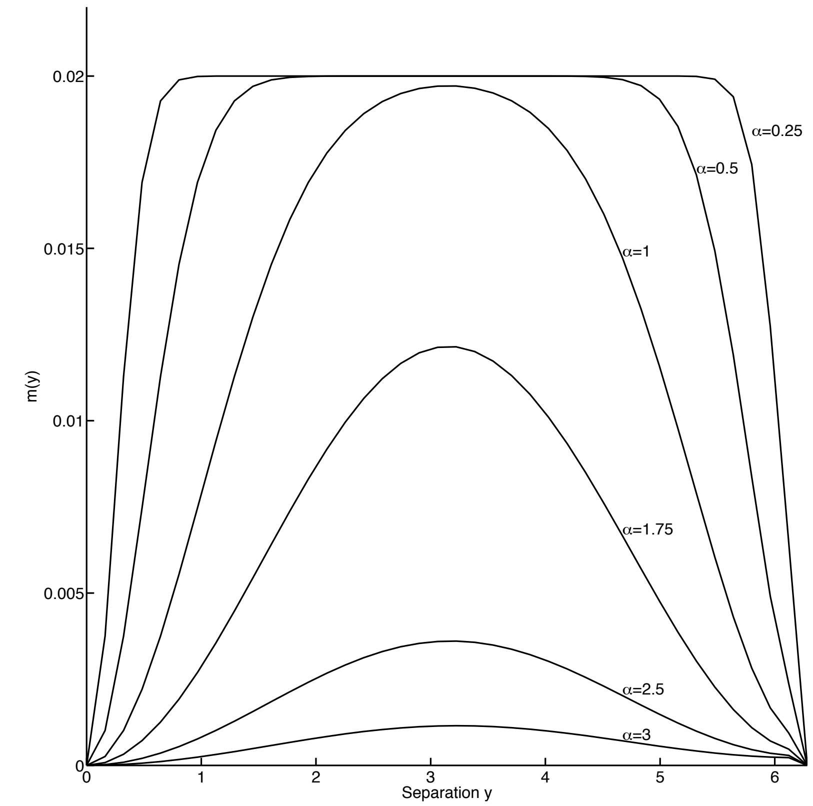

Relative separation $Y_t = X_t^{(1)} - X_t^{(2)}$ solves

$$dY_t = 2\sqrt{C(0) - C(Y_t)}dB_t$$

Generic clumping of deterministic walkers in random environment

For small Y:

$$dY_t \approx c_0 Y_t dB_t,$$

Geometric Brownian Motion, which goes to zero almost surely.

Share price model for volatile return rates...like pension fund

Energy decay

Energy in mode 1 $= \mathbb{E}|a_1^+|^2/|a_1|^2$ Total Energy $= \sum_{k=0}^{\infty} k\mathbb{E}|a_k^{\pm}|^2/|a_1|^2$

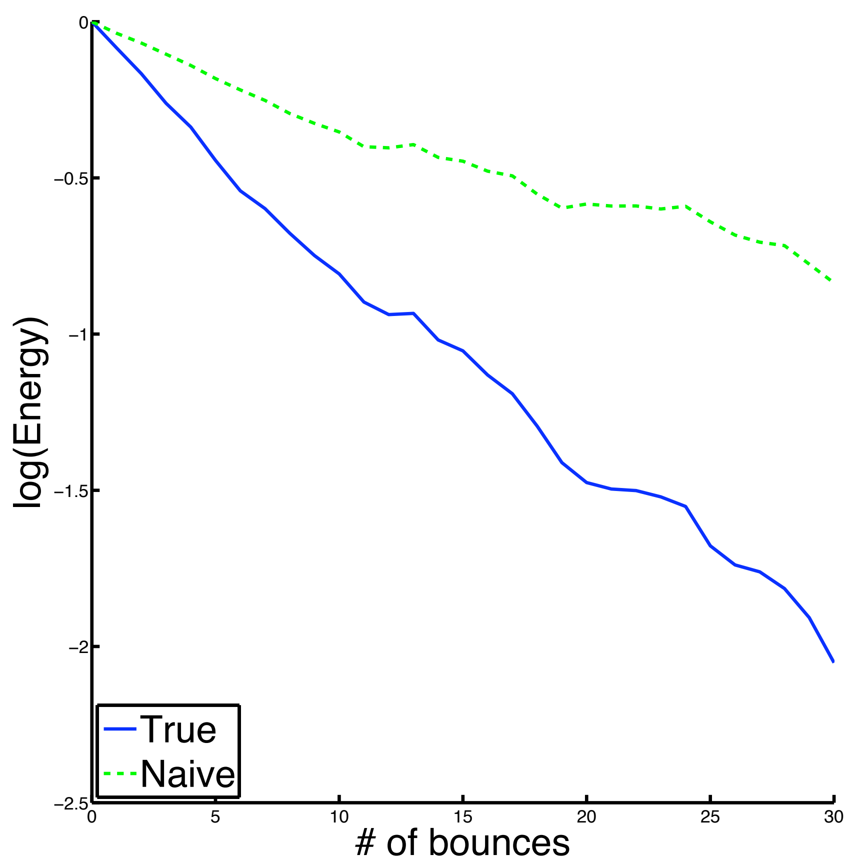

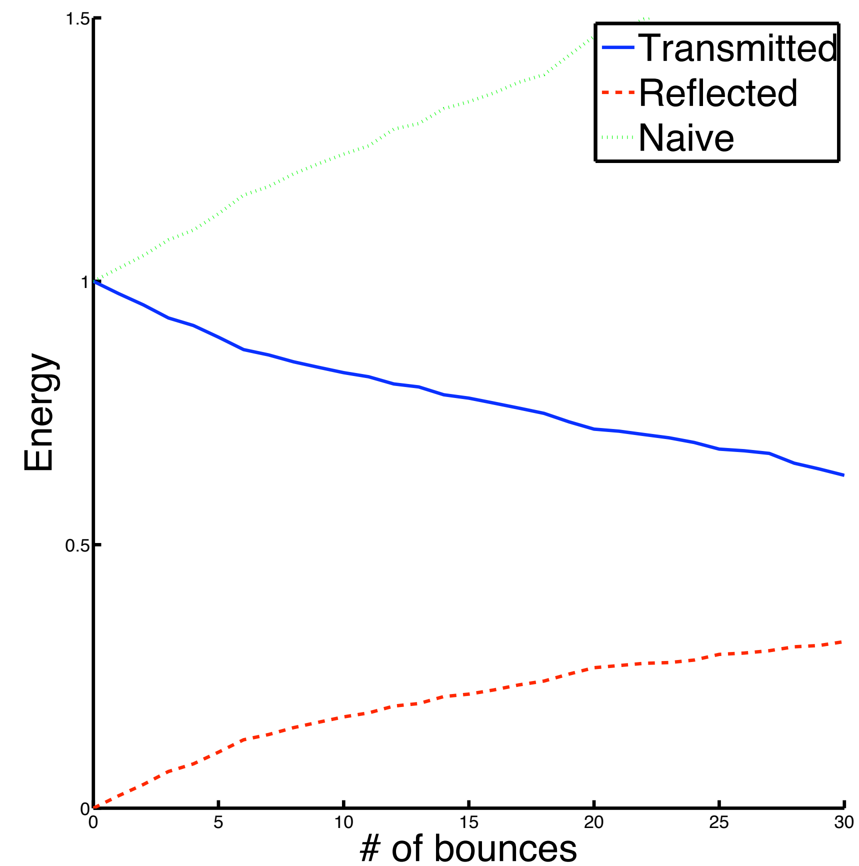

Let $\mathbb{E}|a_1^+|^2 = |a_1|^2 e^{-\lambda_1 b}$, $\mathbb{E}|a_1^{(n)}|^2 = |a_1|^2 e^{-\lambda_1^{(n)} b}$

How do $\lambda_1, \lambda_1^{(n)}$ depend on law of topography?

Scaling laws for uncorrelated topography

$$h(x) \longrightarrow \sigma h(x/\alpha)$$

2 parameters: σ, α

Equivalently σ, σ_D where $\sigma^2 = \mathbb{E}h^2, \quad \sigma_D^2 = \mathbb{E}h_x^2 \propto \frac{\sigma^2}{\alpha^2}$

$C(x) = \sigma^2 e^{-\frac{1}{2}(\frac{x}{\alpha})^2}$

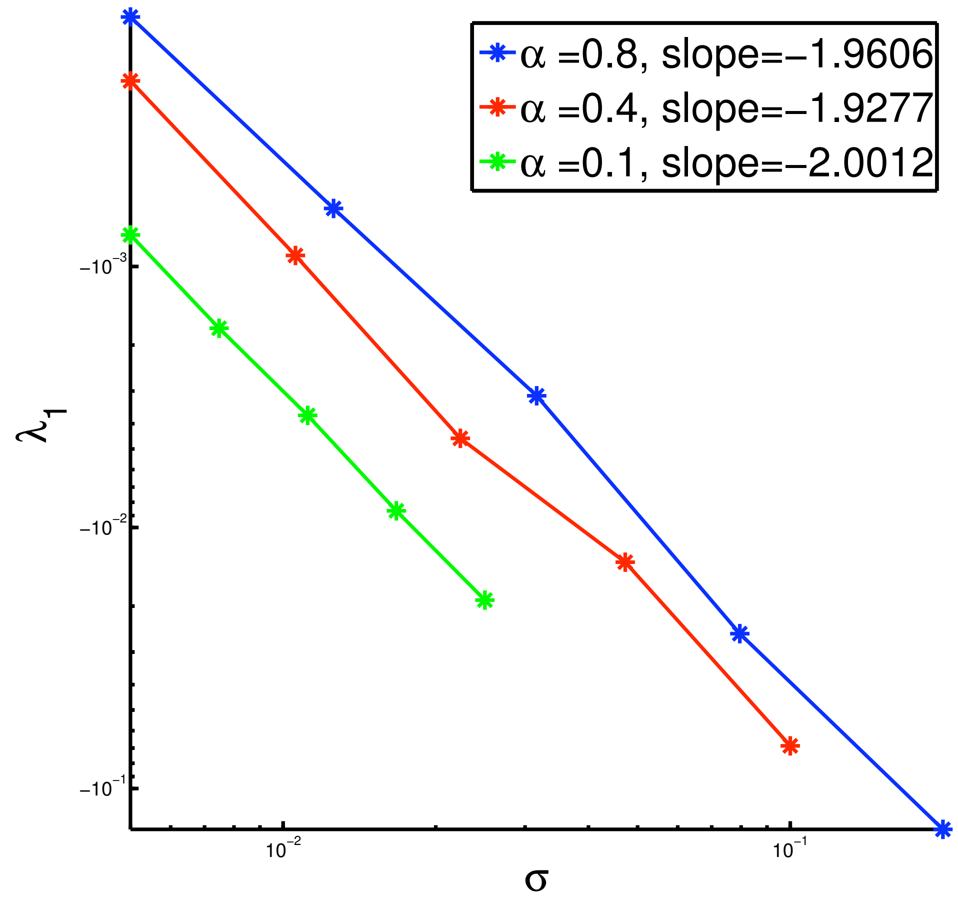

True

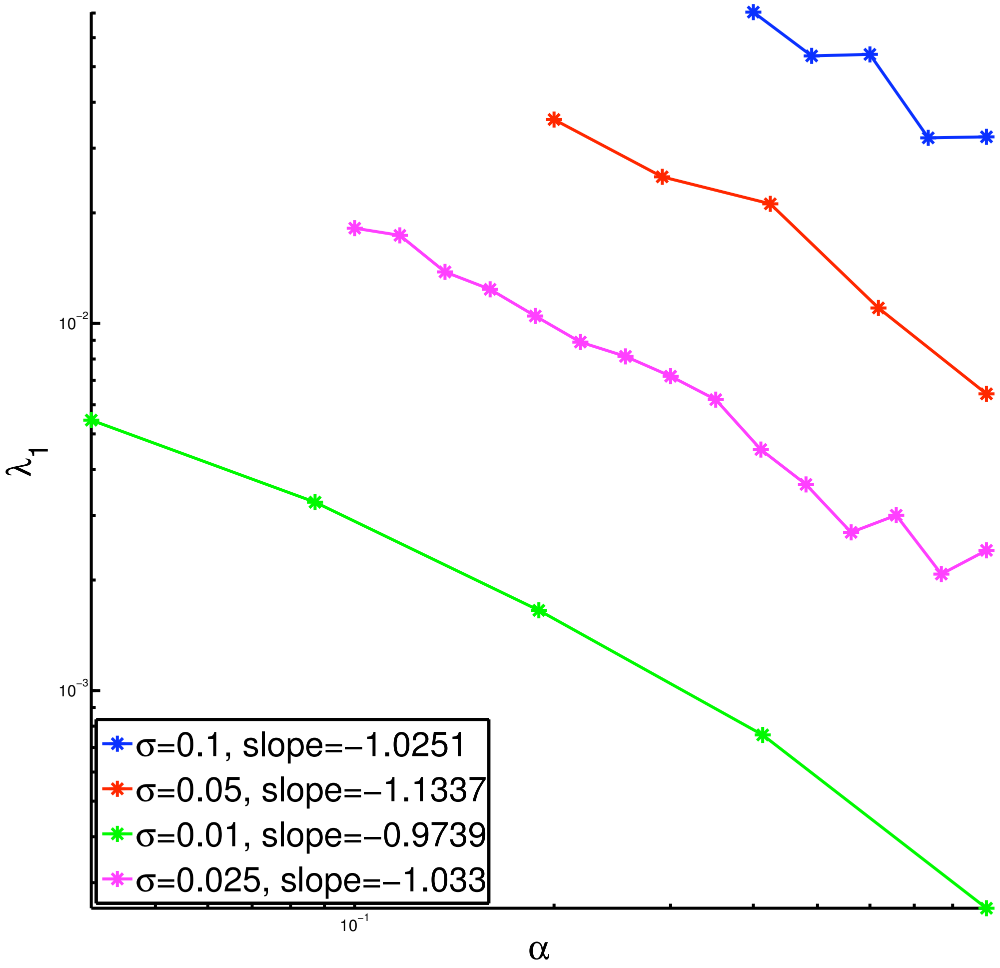

Dimensional result & power law topography

$$\text{dimensional e-folding length} = \frac{2}{C_0}\frac{H^2}{\pi}\frac{1}{\sqrt{\mathbb{E}|h_0|^2}\sqrt{\mathbb{E}|h_0'|^2}}$$

- valid for uncorrelated topography
- $C_0 \approx 2.3$ from numerical simulations
- independent of wave slope $\mu = \sqrt{\frac{\omega_0^2 - f^2}{N^2 - \omega_0^2}}$

For uncorrelated topography Gaussianity assumption does not matter

Values of wave frequency, buoyancy frequency, or Coriolis frequency do not affect the decay length!

Bell: $\mathbb{E}|h_0|^2 = (125\text{m})^2, \qquad \mathbb{E}|h_0'|^2 = (0.14)^2$

Formula for uncorrelated topography

$$\text{dimensional e-folding length} = \frac{2}{C_0}\frac{H^2}{\pi}\frac{1}{\sqrt{\mathbb{E}|h_0|^2}\sqrt{\mathbb{E}|h_0'|^2}} = 250\text{km}$$

Rough topography is an efficient wave decay mechanism

For realistic southern ocean topography obtain a decay scale of 1200 km.

Energy exchange between waves and vortices

Joint work with Marija Vucelja

Interested in energy exchanges without topography and without wave breaking (no smoking gun).

Two types of energy transfer:

wave-wave and wave-vortex

Related questions:

Shape of the wave energy spectrum?

Are waves a net energy source or sink for the vortex flow?

Can’t use ray tracing for ocean applications because vortex scale is only 50km.

Do-be-do-be-doo: shallow water

Single layer of hydrostatic incompressible fluid

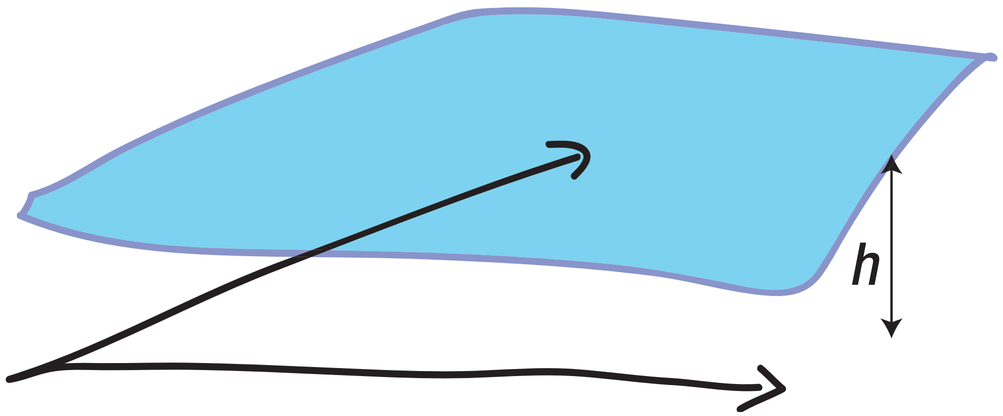

depth h

$$\boldsymbol{x} = (x, y) \qquad \boldsymbol{u} = (u, v) \qquad \frac{\mathrm{D}}{\mathrm{D}t} = \frac{\partial}{\partial t} + (\boldsymbol{u} \cdot \boldsymbol{\nabla})$$

$$\frac{\mathrm{D}\boldsymbol{u}}{\mathrm{D}t} + g\boldsymbol{\nabla} h = 0 \qquad \frac{\mathrm{D}h}{\mathrm{D}t} + h\boldsymbol{\nabla} \cdot \boldsymbol{u} = 0$$

Potential vorticity $q = \dfrac{\boldsymbol{\nabla} \times \boldsymbol{u}}{h}$ such that $\dfrac{Dq}{Dt} = 0$

Linear equations and wave energy

Steady low-Froude number flow s.t. $H \approx \text{const} \quad \text{and} \quad \boldsymbol{\nabla} \cdot \boldsymbol{U} = 0$

Linearized perturbations s.t. h=H+h' and so on:

$$\mathrm{D}_t \boldsymbol{u}' + g\boldsymbol{\nabla} h' = -(\boldsymbol{u}' \cdot \boldsymbol{\nabla})\boldsymbol{U}$$

$$\mathrm{D}_t h' + H\boldsymbol{\nabla} \cdot \boldsymbol{u}' = 0 \qquad \mathrm{D}_t = \frac{\partial}{\partial t} + \boldsymbol{U} \cdot \boldsymbol{\nabla}$$

Disturbance energy and energy exchange term:

$$E = \frac{1}{2}\left(H|\boldsymbol{u}'|^2 + gh'^2\right) \qquad \mathrm{D}_t E + \boldsymbol{\nabla} \cdot (gh'\boldsymbol{u}') = -\underline{H\boldsymbol{u}'\boldsymbol{u}' \boldsymbol{:} \boldsymbol{\nabla}\boldsymbol{U}}$$

ymmv...

Investigate dynamics in doubly periodic geometry

Pseudoenergy for shallow water

Arnold 67, Shepherd 90, Salmon 98

Steady basic flow:

symmetry with respect to time induces an exact conservation law for the disturbance fields, which can be made quadratic at small wave amplitude.

Recipe:

start with exact integral conservation laws for total energy and PV:

$$\mathcal{H} = \int \frac{1}{2}\left(h\boldsymbol{u}^2 + gh\right)\, dxdy \qquad \mathcal{A} = \mathcal{H} + \mathcal{C}$$

$$\mathcal{C} = \int hC(q)\, dxdy, \quad \text{where} \quad q = \frac{\boldsymbol{\nabla} \times \boldsymbol{u}}{h}$$

Here C(q) is a function to be chosen smartly

Pseudoenergy cntd.

Now pick C(q) such that $\delta\mathcal{H} = -\delta\mathcal{C} \quad \Rightarrow \quad \delta\mathcal{A} = 0$

holds for the first variations at the steady basic state.

The structure of that state is given by (valid for any Froude number)

$$\boldsymbol{\nabla}\cdot(H\boldsymbol{U}) = 0 \quad \Rightarrow \quad HU = -\Psi_y \quad \text{and} \quad HV = +\Psi_x.$$

PV conservation along streamlines:

$$Q = \frac{\boldsymbol{\nabla}\times\boldsymbol{U}}{H} = \frac{1}{H}\boldsymbol{\nabla}\cdot\left(\frac{\boldsymbol{\nabla}\Psi}{H}\right) = f^{-1}(\Psi) \quad \Rightarrow \quad \Psi = f(Q)$$

First variation condition then
leads to Arnold's famous result:

$$\boxed{C'(Q) = \Psi = f(Q)}$$

Important
special case: $\Psi = -\lambda Q \quad \Rightarrow \quad C(Q) = -\dfrac{\lambda}{2}Q^2$ Enstrophy

Simple steady basic flows

From now on: $$g = H = 1 \quad \text{and} \quad |\boldsymbol{U}| \ll 1$$

Sinusoidal shear flow:

$$\Psi = \sin y, \quad Q = \nabla^2 \Psi = -\sin y \quad \Rightarrow \quad \lambda = 1$$

4-vortex flow:

$$\Psi = \sin x \sin y, \quad Q = \nabla^2 \Psi = -2 \sin x \sin y \quad \Rightarrow \quad \lambda = \frac{1}{2}$$

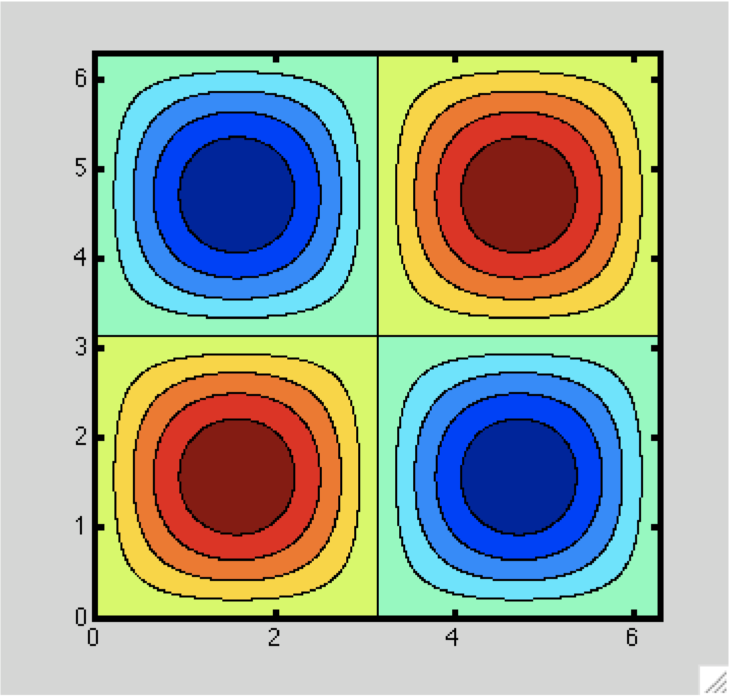

4-vortex flow combines vorticity and strain, good!

It's also unstable to a large-scale vortical disturbance...

Pseudoenergy at second order

Pseudoenergy at second order in disturbance amplitude and small Froude number:

$$\boxed{\mathcal{A} = \int \{ \underbrace{\frac{1}{2}\left(|\boldsymbol{u}'|^2 + h'^2\right)}_{=E} + h'\boldsymbol{u}' \cdot \boldsymbol{U} + \frac{\lambda}{2}\left[h'^2|\boldsymbol{\nabla} \times \boldsymbol{U}|^2 - |\boldsymbol{\nabla} \times \boldsymbol{u}'|^2\right] \}\, dxdy}$$

Wave-vortex energy transfer: can E grow without bound if A is conserved?

Note that: $|h'\boldsymbol{u}'| \leq E \quad \text{because} \quad 0 \leq (|\boldsymbol{u}'| - |h'|)^2$

For small Froude number this means the second term cannot balance unbounded growth of E. This leaves only the vorticity term.

Not relevant to nearly irrotational SW waves. Relevant to vortical instability of basic flow (eg 4-vortex flow), but not of interest here.

Conclusion: wave-vortex energy transfer in SW for steady basic flows is bounded by the Froude number. No such a priori limit for wave-wave transfer.

Numerical model

Two numerical models, one based on (h’,u’,v’) the other based on modal amplitudes for SW without mean flow.

The second one can integrate much faster in time, once it has been debugged...

Both models work in Fourier space and deal with terms such as u’U_x pseudo-spectrally with appropriate dealiasing.

Examle:
basic flow chosen as either shear flow or 4-vortex flow.

Monochromatic initial wave conditions are chosen such that

$$h'(x,y,0) \quad \text{and} \quad \boldsymbol{u}'(x,y,0) = \boldsymbol{\nabla}\phi'(x,y)$$

are isotropic random functions constrained such that the Fourier coefficients are close to a fixed wavenumber kappa_0 = 6

Still a scale separation, but not a slowly varying wavetrain.

Shear flow Fr = 0.5 initial condition

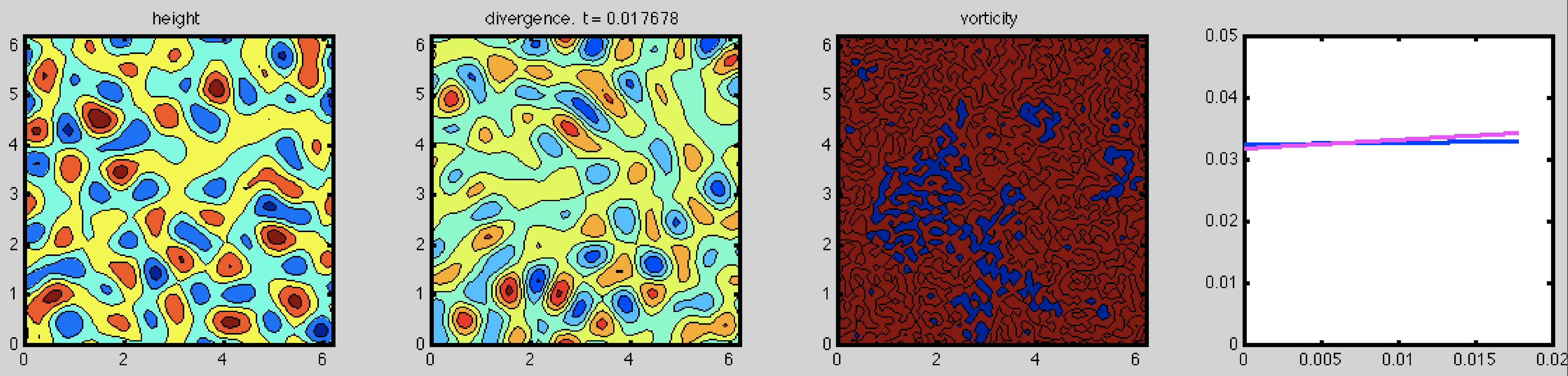

Shear flow Fr = 0.5: t=200

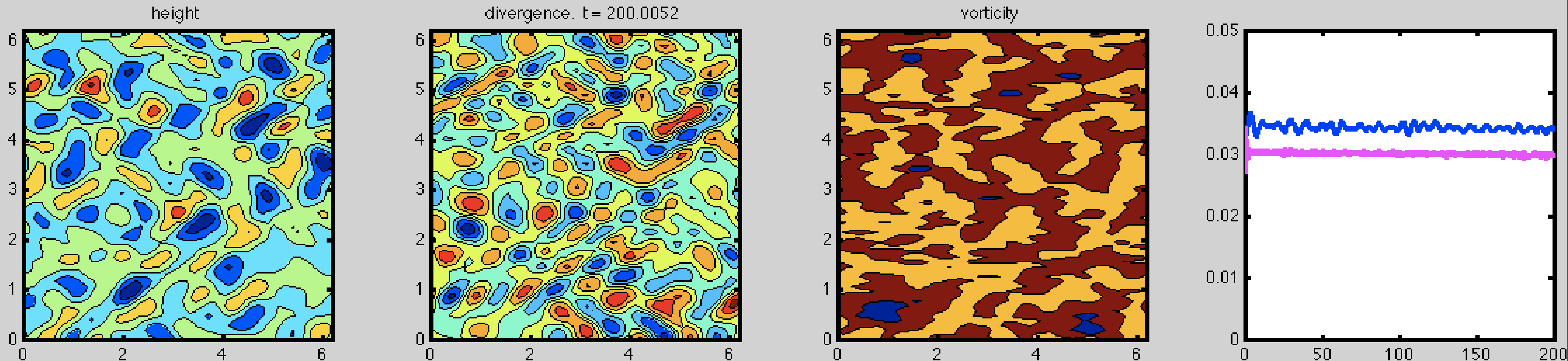

4-vortex flow F=0.5: t=100

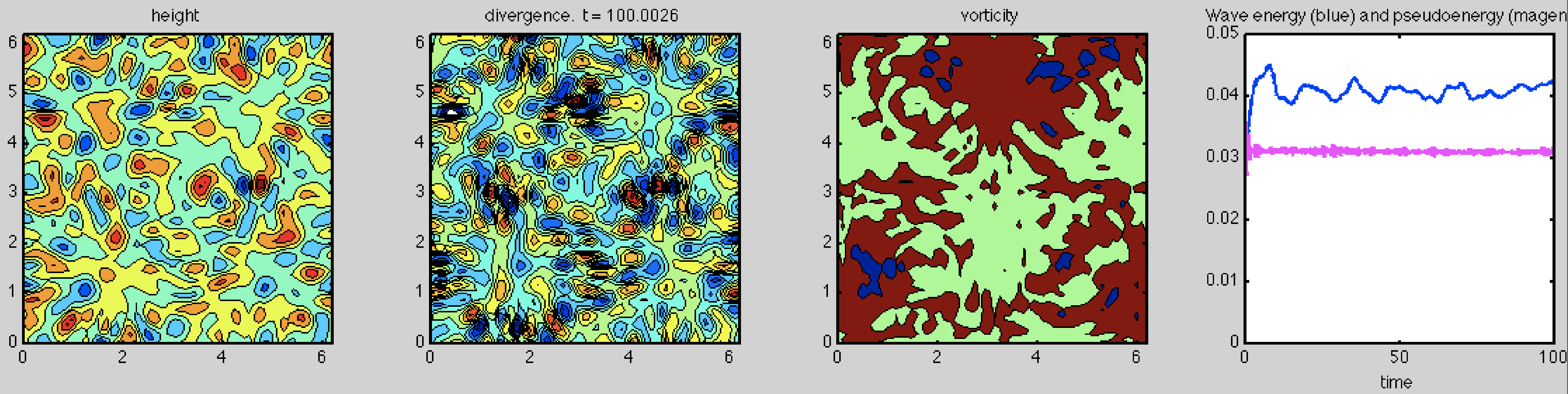

Concluding remarks

Unified numerical modelling of atmosphere and ocean should go with unified thinking about gravity waves